*Quaternary Research*

doi:10.1017/qua.2018.107

# Geochronology, paleogeography, and archaeology of the Acheulian locality of 'Evron Landfill in the western Galilee, Israel

Maayan Shemer[a]*, Onn Crouvi[b], Ron Shaar[c], Yael Ebert[c], Ari Matmon[c], ASTER Team[d], Liora Kolska Horwitz[e], Véra Eisenmann[f], Yehouda Enzel[c], Omry Barzilai[a]

[a]Archaeological Research Department, Israel Antiquity Authority, P.O. Box 586, Jerusalem, Israel
[b]Geological Survey of Israel, 30 Malkhei Israel Street, Jerusalem 9550, Israel
[c]The Fredy and Nadine Herrmann Institute of Earth Sciences, The Edmond J. Safra Campus, The Hebrew University of Jerusalem, Givat Ram, Jerusalem 91904, Israel
[d]ASTER Team: M. Arnold, G. Aumaître, D. Bourlès, K. Keddadouche Centre Européen de Recherche et d'Enseignement de Géosciences de l'Environnement, Unité mixte de recherche 6635 Centre national de la recherche scientifique-Aix-Marseille University, BP 80, 13 545 Aix en Provence Cedex 4, France
[e]National Natural History Collections, Faculty of Life Sciences, The Edmond J. Safra Campus, The Hebrew University of Jerusalem, Givat Ram, Jerusalem 91904, Israel
[f]Unité mixte de recherche 5143 du Centre national de la recherche scientifique, CP 38, Département Histoire de la Terre, 8 rue Buffon, 75005 Paris, France

(Received March 13, 2018; Accepted August 20, 2018)

**Abstract**

A multidisciplinary study was conducted in a newly discovered Paleolithic locality, named 'Evron Landfill. This locality is a part of the Lower Paleolithic complex of 'Evron located at the western Galilee, Israel. Examination of artifacts has enabled the cultural attribution of 'Evron Landfill to the Early Acheulian, while detailed paleomagnetic stratigraphy places the hominin occupations near the Brunhes–Matuyama transition ~0.77 Ma. This age is constrained by cosmogenic isotope burial dating of the sediments overlying the Paleolithic finds, providing a minimum age of ~$0.66 \pm 0.11$ Ma for hominin activity at the site. These results are further supported by the biochronological information derived from the faunal assemblage. Comparative analyses of faunal remains and lithic artifacts from 'Evron Landfill demonstrate similarities to the assemblages from the Early Acheulian site of Evron Quarry, located ~300 m to the south. Pedo-sedimentological analyses indicate that hominin activity took place in a marsh environment in proximity to the Mediterranean coast, which probably fluctuated in both space and time with a fluvial environment. In addition, this study provides important data about ancient coastal activity during the early to middle Pleistocene.

**Keywords:** Lower Paleolithic; 'Evron; Acheulian; Ancient coast; Western Galilee; Soil stratigraphy; Paleomagnetic stratigraphy; Cosmogenic isotope burial age

## INTRODUCTION

The southern Levant (comprising modern-day southern Syria, Lebanon, Jordan, Israel, and the Sinai Peninsula of Egypt), is a narrow strip of land, constrained by the Mediterranean Sea to the west, and dry steppe or deserts (the Negev, Sinai, and Arabia) to the south and in the hinterland east of the Jordan Valley. This region forms a natural land passage between Africa and Eurasia and has played a major role in early hominin dispersal, probably functioning as a conduit into Asia and Europe, as attested by some of the earliest evidence of hominin occupations outside of Africa (Aguirre and Carbonell, 2001; Bar-Yosef and Belfer-Cohen, 2001; Saragusti and Goren-Inbar, 2001; Templeton, 2002; Goren-Inbar and Speth, 2004; Gunz et al., 2009; Sharon, 2014).

Lower Paleolithic (LP) sites in the southern Levant are located in a variety of geographic settings, but share common characteristics: most are located in open landscapes and are consistently situated near freshwater sources (Stekelis and Gilead, 1966; Gilead and Israel, 1975; Gilead and Ronen, 1977; Bar-Yosef and Goren-Inbar, 1993; Guérin et al., 1993; Ronen, 1993; Ronen and Winter, 1997; Rollefson et al., 1997; Shea, 1999; Goren-Inbar et al., 2000; Barzilai et al., 2006; Rollefson et al., 2006; Horwitz and Chazan, 2007; Rech et al., 2007; Malinsky-Buller et al., 2011; Marder et al., 2011; Lister et al., 2013). An additional characteristic common to these sites is the composition of the faunal assemblages, demonstrating the preferential exploitation of medium to large-sized mammals and, in some

*Corresponding author at: Archaeological Research Department, Israel Antiquity Authority, POB 586, Jerusalem, Israel. E-mail address: Shemerma@hotmail.com (M. Shemer).

cases, extremely large-sized mammals such as elephant and hippopotamus (Yisraeli, 1967; Tchernov, 1987; Horwitz and Tchernov, 1989; Tchernov, 1992, Tchernov et al., 1994; Goren-Inbar et al., 1994; Horwitz and Monchot, 2007; Martínez-Navarro et al., 2009; Rabinovich et al., 2011; Yeshurun et al., 2011; Rabinovich et al., 2012; Lister et al., 2013). The observed settlement patterns demonstrate repeated visits to favored localities (Gilead and Ronen, 1977; Goren-Inbar and Speth, 2004; Barzilai et al., 2006; Horwitz and Chazan, 2007; Goring-Morris et al., 2009; Marder et al., 2011; Bar-Yosef and Belfer-Cohen, 2013). There is also evidence for cave exploitation, mostly characterizing the late LP (e.g., Neuville, 1951; Garrod, 1956, 1970; Jelinek, 1990; Weinstein-Evron et al., 1999, 2003; Gopher et al., 2005, 2010; Valladas et al., 2013).

Culturally, most of the LP open-air occupations in the southern Levant are ascribed to the Acheulian techno-complex. This lithic tradition is typically associated with the production and use of bifacial tools, of which hand axes and cleavers are the most well-known types (e.g., Gilead, 1970; Debénath and Dibble, 1994; Sharon, 2007; Herzlinger et al., 2017). Today, a division of the Levantine Acheulian techno-complex into three or four phases (where the Acheulo-Yabrudian marks the final phase) is generally accepted, corresponding to environmental changes as well as technological and quantitative differences observed within and between assemblages (Bar-Yosef, 1994; Sharon, 2014).

The absolute dating of Acheulian occupations and their attribution to a specific cultural phase is a challenging task, mainly due to the fact that few absolute dating methods can reach back further than 0.5 Ma. Worldwide, the most reliable ages for LP sites are bounded by K-Ar/Ar-Ar dating of overlaying and/or underlying volcanic strata (e.g., Goren-Inbar et al., 1992; Mishra et al., 1995; Porat et al., 1999; Barkai et al., 2003; Coltorti et al., 2005; Norton et al., 2006). These strata are rare in the southern Levant, however, and are absent in most Acheulian contexts in this region, with the exception of the site of Gesher Benot Ya'akov (Goren-Inbar et al., 1992). In many of the early excavations, site chronology relied upon biostratigraphy and lithic technological and typological analyses (e.g., Bar-Yosef, 1994; Tchernov et al., 1994 and references therein). Nowadays, a suite of advanced dating techniques can provide ages for older time spans (e.g., TT-OSL, pIR-IR290, cosmogenic isotope burial age, and paleomagnetic stratigraphy), thus allowing the reconstruction of a more reliable chronometric framework for the LP in the southern Levant (e.g., Porat et al., 2002; Porat and Ronen, 2002; Malinsky-Buller et al., 2016; Zaidner et al., 2018).

At the center of this paper is a complex of Acheulian sites located near Kibbutz ‘Evron (western Galilee, Israel; Fig. 1). Seven distinct localities, representing various phases of the Acheulian techno-complex, have been discovered to date at ‘Evron, implying that this environment was a favorable setting for hominin activity during the LP (Stekelis, 1950; Prausnitz, 1969; Gilead and Ronen, 1977; Ronen, 1991, 1993). The sites are situated ~400 m north of the Beit Ha'emeq stream, which drains the western Galilee Mountains into the Mediterranean Sea. More specifically, this area is situated in an alluvial plain (~30 m above sea level [asl]), accreted between a prominent eolianite (kurkar) ridge, ~40 m asl, running parallel and 1.5–2 km east of the current shoreline and the Galilee Mountains (Fig. 1). The exact location of some of the LP localities in this complex is unclear, as many were found by amateur archaeologists who did not systematically document their position. Figure 1 presents the estimated location of some of the ‘Evron sites, based on relevant published data (Stekelis, 1950; Gilead and Ronen, 1977; Ronen, 1991, 1993).

The most well-known site in the ‘Evron complex, and the one most extensively excavated and studied to date, is Evron Quarry, considered to represent an early Acheulian occurrence based on lithic analyses (Ronen and Prausnitz, 1979; Gilead and Ronen, 1977; Ronen, 1979; Ronen, 1991; Chazan, 2013). Discovered in a once-active eolianite quarry, this site was interpreted as a series of repeated occupations, as was demonstrated by three distinct archaeological layers (Ronen and Prausnitz, 1969; Ronen, 1991). The lithic industry from Evron Quarry includes coarse hand axes and chopping tools (Gilead and Ronen, 1977) as well as a small-flake industry (Chazan, 2013). The faunal assemblage yielded remains of two Proboscideans - *Elephas* sp. and *Stegodon* sp., as well as an endemic suid *Kolpochoerus evronensis*, *Hippopotamus amphibus*, *Cervus elaphus*, *Bos* cf. *primigenius*, *Gazella* cf. *gazella*, *Capreolus* sp., a hyaenid, *Gerbillus*, and *Trionyx* (Haas, 1970; Ronen and Prausnitz, 1979; Tchernov et al., 1994).

Based on comparative analyses of lithic and faunal assemblages, the age of Evron Quarry was initially estimated to range between 1.0–0.8 Ma (Gilead and Ronen, 1977; Ronen, 1991; Tchernov et al., 1994). In the late 1990s, site chronology was established using optically stimulated luminescence (OSL), electron spin resonance (ESR), and paleomagnetic stratigraphy of sediments from trench-sections dug in an adjacent field and from an exposed 5-m-deep section, located some 500 m northeast of the original site (Porat and Ronen, 2002; Ron et al., 2003). OSL and ESR results yielded a minimum age of 0.50–0.65 Ma for the geological unit that is assumed to correspond to the archaeological layer (Porat and Ronen, 2002), while the paleomagnetic stratigraphy constrained its age between the Jaramillo subchron and the Brunhes/Matuyama transitions. This points to a time of deposition sometime during the interval of 1.0–0.8 Ma, similar to the initial chronology that was suggested based on regional comparative analyses of the lithic and faunal assemblages (Ron et al., 2003). Since absolute ages were retrieved from off-site sections, however, these ages relied on a correlation between geological units in the trenches, the exposed section and in the archaeological site. Therefore, their association to the excavated archaeological layers is considered by many as insecure.

During October 2014, a massive construction operation was initiated ca. 300 m northwest of the Evron Quarry site.

https://doi.org/10.1017/qua.2018.107 Published online by Cambridge University Press

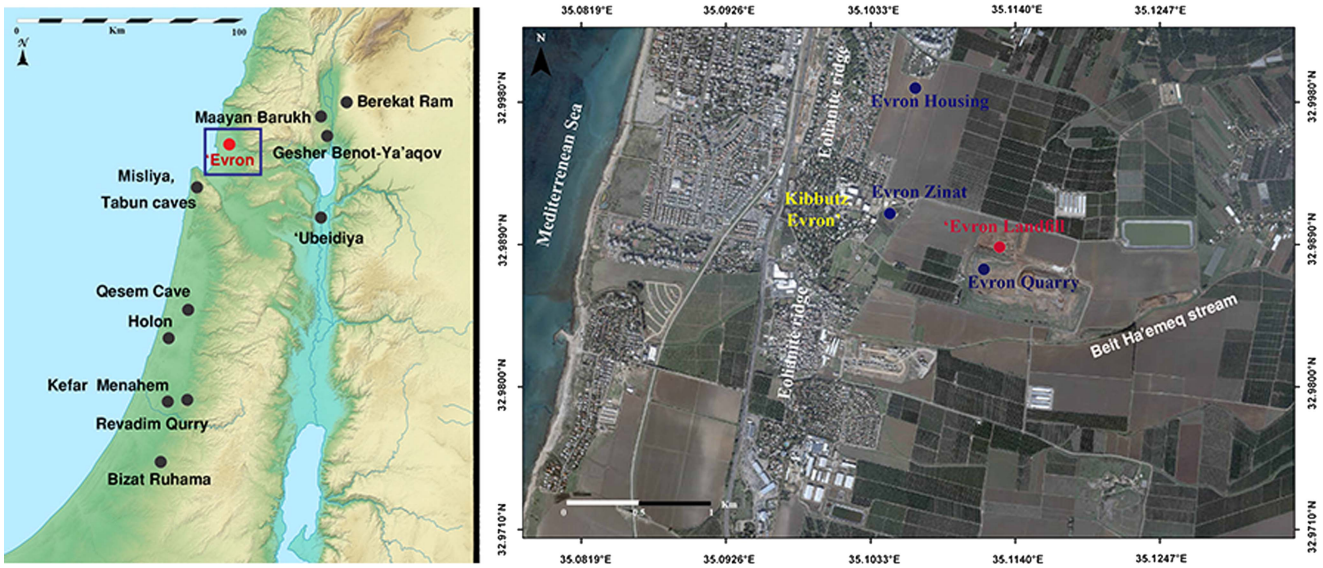


**Figure 1.** (color online) Main Lower Paleolithic sites in Israel over topographic map. Enlarged: Estimated location of selected sites in the 'Evron complex, including the newly found locality of 'Evron Landfill.

Large-scale earthworks exposed a deep (~14 m) sedimentary sequence, revealing a complex stratigraphy of the ancient Mediterranean coastal plain (Shemer and Barzilai, 2017). Animal bones and flint artifacts were identified at depths of 9–11 m, originating from a red clayey sediment, indicating the possible presence of a new Acheulian occurrence within the Evron site complex (henceforth 'Evron Landfill; Fig. 1).

Based on a multidisciplinary study conducted on-site at the 'Evron Landfill locality that incorporated archaeological, geological, and paleomagnetic stratigraphy analyses, as well as dating of the archaeological layer based on cosmogenic isotope burial age, we introduce new data regarding the chronological framework and depositional environments of the Acheulian complexes near 'Evron.

## METHODS

### Site settings and the archaeological excavation

During October 2014, massive earthworks aiming to expand the landfill operating in the quarry grounds since the 1990s were initiated in the fields to its north. These included a large-scale digging operation using heavy machinery, covering an area of ca. 4 ha and designated to reach a maximum depth of 19 m below the surface. Due to safety considerations and in order to prevent collapses, the walls of this pit were artificially stepped, with each step reaching a maximum depth of 2–3 m (Supplementary Figures 1–6).

Upon reaching a depth of 9–11 m, animal bones and flint artifacts were discovered embedded in red clayey sediments. Following this discovery, a series of test trenches were dug using a JCB backhoe, indicating the possible existence of concentrations of archaeological finds in the western part of the landfill. Archaeological excavations were then conducted, focused on four of the trenches (T1–T4; Fig. 2). The trenches were subjected to manual section cleaning in search of an archaeological layer. *In situ* finds were discovered only in T2, leading to the opening of 1 × 1-m excavation square at its southern edge (Shemer and Barzilai, 2017). All sediments were dry sieved using a 10-mm mesh.

### Soil stratigraphy and pedo-sedimentry units

The soil stratigraphy of the 'Evron Landfill was determined based on detailed description and sampling of three pedo-sedimentary sequences, following standard procedures (Soil Survey Staff, 1999). Two of the documented sequences are located on the eastern and western edges of the landfill, and are termed Eastern and Western sequences, respectively (Fig. 2 and 3). Due to the artificial, stepped morphology of the landfill walls, the units were described and sampled along a ~30 m horizontal strip. The third sequence (termed the Central-Southern sequence) is composed of two sections: the base of the sequence (termed the Central sequence) was sampled in Trench T2 (the main archaeological excavation area; Fig. 2) and in an exposed section located ~30 m west of the trench. The top of the sequence was sampled in the southern wall of the landfill (termed the Southern sequence). The correlation between the Central and the Southern sequences was carefully inspected and validated in the field, and thus they are reported here as a single continuous sequence (Central-Southern sequence).

The coordinates and elevation of the unit boundaries for each sequence were determined using a RTK-GPS device. Correlations between the sequences and lateral changes within the units are based on field observations along the exposed landfill walls. Based on the above, two schematic cross sections were constructed for the entire landfill (Fig. 2 and 3); one from WNW to ESE (A–A′) and the second from SSW to NNE (B–B′).

https://doi.org/10.1017/qua.2018.107 Published online by Cambridge University Press

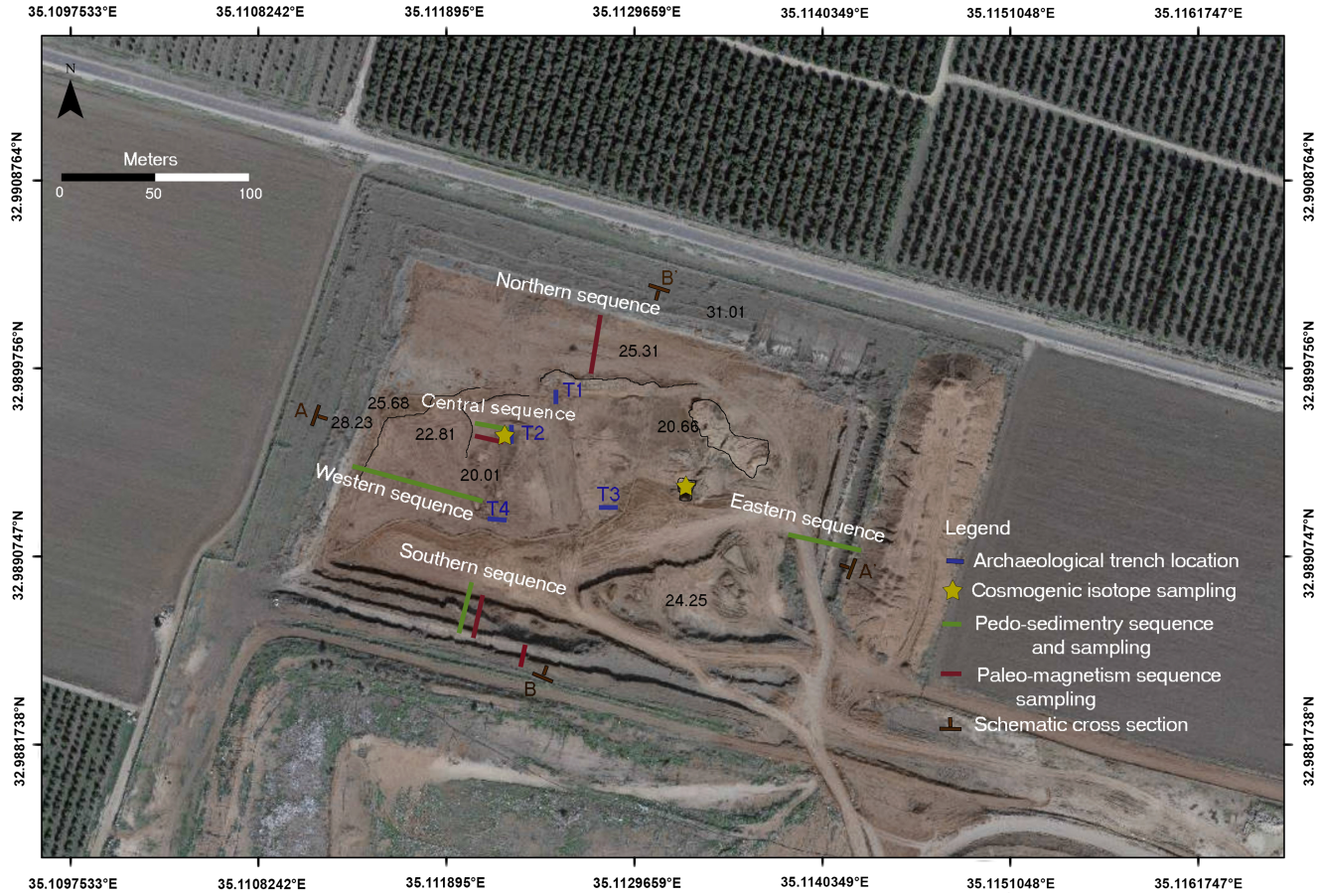


**Figure 2.** (color online) 'Evron Landfill sampling locations. Numeric values indicate elevation (m) above sea level.

The sediment samples were oven dried, divided and sieved through 2-mm mesh. All samples were analyzed for bulk particle-size distribution (PSD) using Malvern MS-2000 laser diffraction device, following the procedure of Crouvi et al. (2008). Samples from three units were examined for micromorphology using thin sections.

## Paleomagnetic stratigraphy

Within the framework of the paleomagnetic study, 101 oriented samples were collected from 26 different sedimentary horizons in the Southern, Central, and Northern sequences (Fig. 2 and 3 and Supplementary Material) in a twofold effort: (a) to construct a magnetostratigraphic age model of the site, and (b) to cross-correlate the sedimentary units in the three sequences. From each horizon, three oriented samples were collected for alternating field (AF) demagnetization experiment using non-magnetic plastic boxes (1.5 × 1.5 × 1 cm). In this method, a cube-shaped sample with three vertical faces and two horizontal faces is carved from the section. After the sediment sample is placed in a plastic box, its orientation is precisely measured. It is then carefully separated from the section and glued within the plastic box using non-magnetic glue. In addition, from all horizons except the three sampled in Trench T2 (Fig. 2), a fourth sample was collected using a quartz cylindrical crucible, measuring 2.54 cm (1 inch) in diameter and height, for thermal demagnetization experiments.

Paleomagnetic experiments were carried out at the paleomagnetic laboratory in the Institute of Earth Sciences, the Hebrew University of Jerusalem, using a 2G-750 superconducting rock magnetometer equipped with in-line 2-axis AF coils, and ASC-TD48 thermal demagnetizer. AF demagnetizations were done at progressively elevated peak magnetic field strength in 5 mT or 10 mT steps up to peak field strength ranging between 50 mT to 120 mT, until the entire magnetization vector was removed. Thermal demagnetizations were done in 50°C steps from 50°C up to 300°C, and in 40°C steps up to 680°C, or until the sample was completely demagnetized. The direction of the characteristic remanence magnetization was determined based on end-point Zijderveld (1967) diagrams using the Demag-GUI program, a part of the PmagPy software package (Tauxe et al., 2016). The polarity sequence was compared with the Quaternary Geomagnetic Instability Time Scale of Singer (2014).

## Cosmogenic isotope burial dating

Cosmogenic isotope burial dating enables the dating of continental sediments over a time range of 0.5–5 Ma and in settings where other dating methods do not apply (Granger and Muzikar, 2001; Granger, 2006; Hidy et al., 2014; Matmon

https://doi.org/10.1017/qua.2018.107 Published online by Cambridge University Press

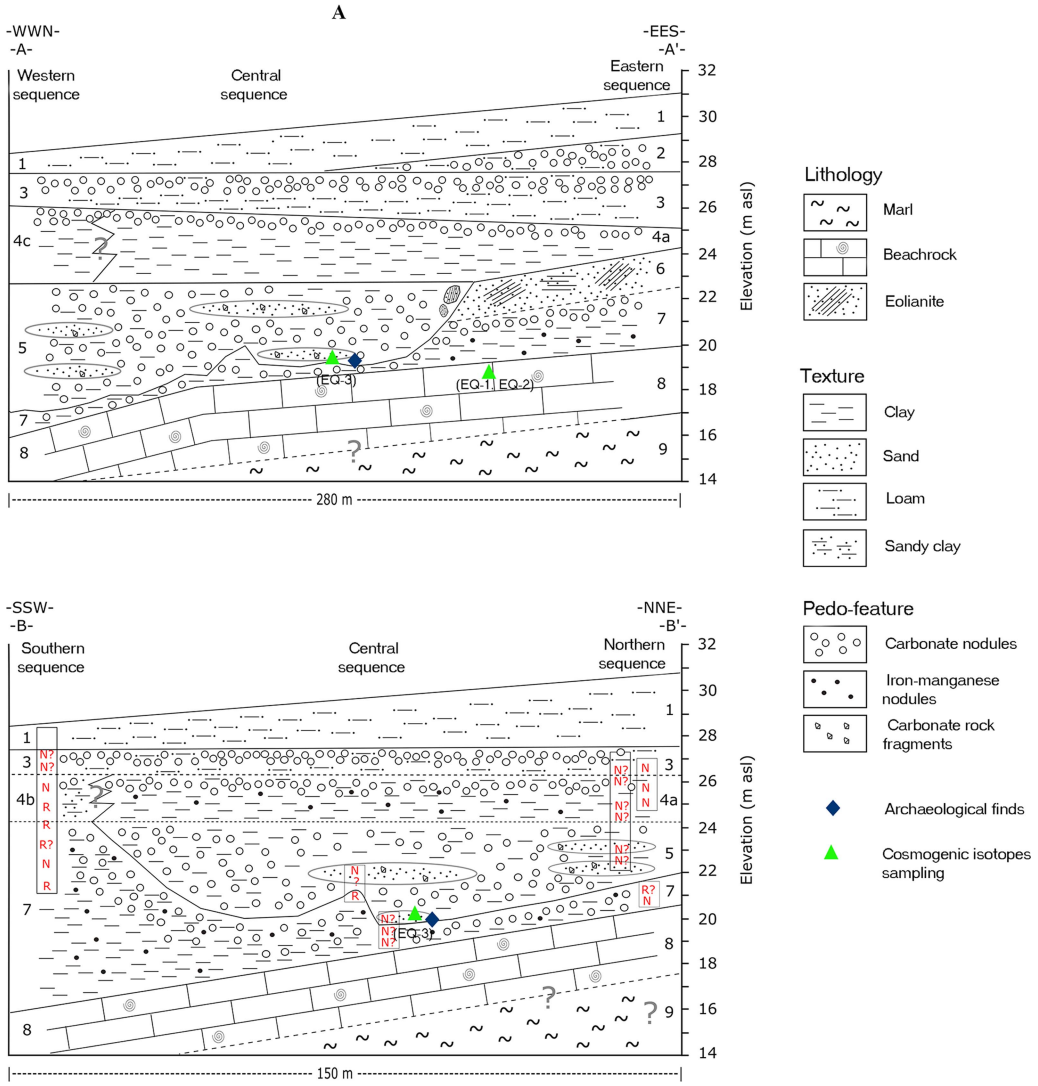


**Figure 3.** (color online) Schematic cross sections (a) WWN-EES and (b) SSW-NNE, with the location of paleomagnetic results.

et al., 2014). $^{10}$Be–$^{26}$Al burial dating of sediment is based on a process in which these two nuclides are produced in a material at, or near, the surface at a known ratio and then buried and shielded from further cosmic-ray bombardment such that production effectively ceases. Once production is shut off, nuclide concentrations are governed by radioactive decay. This ratio decreases with time since $^{26}$Al decays about twice as fast as $^{10}$Be: the half-life of $^{10}$Be is 1.387 Ma (Chmeleff et al., 2010; Korschinek et al., 2010) and the half-life of $^{26}$Al is 0.705 Ma (Nishiizumi, 2004).

The accepted surface production ratio of $^{26}$Al and $^{10}$Be in quartz in most natural settings is ~6.8 ( Nishiizumi et al., 2007; Balco et al., 2008), although recent studies suggest this ratio may vary slightly depending on altitude (Argento et al., 2013; Lifton et al., 2014). Using Equation 1, a simple burial age may be easily calculated (Granger et al., 1997):

$$\left(\frac{N_{26}}{N_{10}}\right)_{(t)} = \left(\frac{N_{26}}{N_{10}}\right)_{(0)} e^{-t_{burial}\left(\frac{1}{\tau_{26}}-\frac{1}{\tau_{10}}\right)} \quad \text{(Eq. 1)}$$

Where $\left(\frac{N_{26}}{N_{10}}\right)_{(t)}$ is the ratio of the measured $^{26}$Al and $^{10}$Be concentrations, $\left(\frac{N_{26}}{N_{10}}\right)_{(0)}$ is the initial ratio of $^{26}$Al and $^{10}$Be concentrations (at the time of burial), $t_{burial}$ is the time since burial, and $\tau_{10}$ and $\tau_{26}$ are the mean lives of $^{10}$Be and $^{26}$Al (Granger and Muzikar, 2001), respectively.

Complications to this simple approach arise if the pre-burial ratio is below that of the production ratio (for example, if there was a previous burial period or if bedrock was exhumed very slowly), or if burial was shallow such that post-burial nuclide production by deeply penetrating muons still occurred. In these cases, either a maximum or minimum age for the case of a significant inherited depositional ratio or post-burial production, respectively, is given, or additional independent constraints are required.

$^{10}$Be–$^{26}$Al burial dating methods can generally be applied to sediments that are buried longer than 0.3 Ma, at which time the measured $^{26}$Al/$^{10}$Be ratio can be reliably distinguished from the surface production ratio. The maximum limit of the method is ~5 Ma, at which time ~7 half-lives of $^{26}$Al reduce its

https://doi.org/10.1017/qua.2018.107 Published online by Cambridge University Press

concentration either to secular equilibrium, which is controlled by the very low production rate of nuclides by deeply penetrating muons, or to a level beneath current accelerator mass spectrometry (AMS) measurement capabilities (Matmon et al., 2014).

Three samples were collected to constrain the burial age of the lower part of the 'Evron Landfill sequence (Fig. 2, Supplementary Figure 1). Samples EQ-1 and EQ-2 were collected from a pit excavated in the middle of the site (Unit 8), where the deepest possible part of the section was exposed. Carbonate cemented eolianite was exposed at the base of the pit (Supplementary Figure 1a); its lower part is massive while the upper part is finely bedded. Sample EQ-1 was collected from the lower massive unit, 12.9 m below the pre-excavation surface, while sample EQ-2 was collected from the layered unit, 12.5 m below the pre-excavation surface. Sample EQ-3 was collected from the main archeological area (Trench 2), closer to the western side of the site (Fig. 2, Supplementary Figure 1b). This sample was collected from a massive red clay unit rich in quartz grains, which correlates with the artifact-bearing Unit 5 in the Central sequence of the landfill. This sample is positioned 10.0 m below the pre-landfill surface.

Measurements of $^{10}$Be and $^{26}$Al were made on the quartz 250–850 µm grain-size fraction. Quartz cleaning procedure and the extraction of Be and Al cations (converted to oxides) followed standard procedures (Kohl and Nishiizumi, 1992; Bierman and Caffee, 2001). Samples were analyzed at ASTER, CEREGE, Aix en Provence, France. Isotopic ratios of $^{10}$Be/Be and $^{26}$Al/Al were corrected with chemistry process blanks and normalized to accepted in-house AMS standard reference materials with agreed nominal isotopic ratios.

## RESULTS

### Soil stratigraphy and pedo-sedimentry units

The 'Evron Landfill presents a ~14 m complex pedo-sedimentary sequence of coastal and on-land, near-coastal sediments, including beach rock, eolianite, sands, and wetland deposits (Fig. 3; Tables 1–3). The entire sequence unconformably overlies yellow marl (not sampled, base not exposed, Unit 9 in Fig. 3). The lowest sampled Unit 8 is a 3-m-thick carbonate-rich beach rock with prominent horizontal bedding and signs of pedogenesis (roots casts and burrowing). A ~30-cm-thick calcrete caps the beach rock. The top of Unit 8 dips to the west and south.

Unit 7 uncomfortably overlies the beach rock with an abrupt and wavy boundary. It is composed of brown sticky clay to silty clay, rich in black iron-manganese nodules. In the eastern wall, a well-developed calcic horizon was observed at the upper part of this unit. Farther west, clear erosional features were identified cutting the top of this unit (see Unit 5).

Unit 6 is a 1.3-m-thick, dull orange eolianite that abruptly overlies the clay sediments of Unit 7. This unit appears only in the eastern part of the landfill. It dips to the west and can be traced towards the central part of the landfill to a point where it is cut by Unit 5.

Unit 5 is composed mostly of brown clay sediments similar to Unit 7, with alternating fluvial layers/lenses rich with sand grains. This unit shows clear cut-and-fill morphologies and cut into Units 7 and 6. The fluvial layers within Unit 5 vary in thickness from a few centimeters to ~0.5 m and are composed of many angular quartz sand grains, with a few carbonate rock fragments; in a few of these fragments Cretaceous foraminifera were identified, meaning these fragments originated east of the site in bedrock exposures. The cement is composed of calcite and iron oxides, and fills small pores between grains, indicating a vadose environment (i.e., water leaching above water level). The erosional contact between Unit 5 and the eolianite of Unit 6 resembles sea-cliff morphology. Eolianite clasts were identified within Unit 5 near the contact between these units. Unit 5 was identified only in the Western, Central and Northern sequences. It thickens to the west.

Unit 4 uncomfortably overlies the eolianite of Unit 6 in the eastern part of the landfill, the fluvial sediments of Unit 5 in the Central and Western parts, and the clay sediments of Unit 7 in the southern part. The characteristics of this unit vary laterally and appear differently in each of the studied sequences. Thus, we cannot assume that this unit is a simple chronostratigraphic unit. In the Eastern sequence, Unit 4 is 1.1-m-thick reddish-brown clay, with a well-developed calcic horizon. In the Central sequence, Unit 4 is thicker (3.3 m) dark-grayish yellow clay, with few iron-manganese nodules and with a well-developed calcic horizon at the top. In the Southern sequence, this unit is bright reddish-brown sandy loam to sandy clay loam, with calcic horizon at the top. The lateral boundaries between these facies comprising Unit 4 were not clearly identified in the field.

Unit 3 abruptly overlies Unit 4. It is composed of 1–2 m-thick, gray silty clay to clay with well-developed calcic horizon at the upper part of the unit.

Unit 2 appears only in the eastern part of the landfill. It is a 2-m-thick bright yellowish-brown loam, with very well-developed calcic nodules. The unit gradually disappears to the west and does not appear in the Central sequence.

Unit 1 abruptly overlies Unit 2 in the eastern part of the landfill and Unit 3 in its western part. It is 1–2.5 m-thick, brownish-black silty clay that caps the entire sequence of the 'Evron Landfill.

Flint artifacts and faunal remains found during the excavation originated from the contact between stratigraphic Units 7 and 5. Most of the finds were collected from the northwestern part of the landfill. During the excavation some sorting of the finds was observed: all animal bones and large artifacts (>5 cm) were embedded in the brown clayey sediment of Unit 7, whereas smaller flint artifacts tended to be more common in the fluvial sediments associated with Unit 5.

### Paleomagnetic stratigraphy

Our criterion for a reliable magnetic polarity interpretation of a horizon (where N stands for normal, and R stands for

https://doi.org/10.1017/qua.2018.107 Published online by Cambridge University Press

**Table 1**. The Eastern pedo-sedimentary (PS) sequence.

| PS unit | Horizon | Depth (m) | Thickness (m) | Description | Sample (Evron-#) |
|---|---|---|---|---|---|
| **1** | Bw | 0–2.0 | 2.0 | Silty clay, brownish-black (2.5Y 3/2), moderate medium subangular blocky structure, moderately sticky, moderately plastic, abrupt and wavy boundary. | 1 |
| **2** | Bkmb | 2.0–4.0 | 2.0 | Loam, bright yellowish-brown (10YR 6/8), common medium irregular strongly cemented sharp carbonate concentrations, gradual and wavy boundary. | 2 |
| **3** | Bkb | 4.0–4.6 | 0.6 | Silty clay, gray (5Y 5/1), moderate medium columnar structure, moderately sticky, moderately plastic, many coarse–very coarse irregular strongly cemented sharp carbonate concentrations, gradual and smooth boundary. | 3 |
| | Bwb | 4.6–5.9 | 1.3 | Clay, gray (5Y 5/1), moderate medium columnar structure, moderately sticky, moderately plastic, abrupt and wavy boundary. | 4 |
| **4a** | Bkb | 5.9–7.0 | 1.1 | Clay, thick reddish-brown (5YR 4/6), moderate medium-coarse subangular blocky structure, very sticky, very plastic, common coarse irregular strongly cemented sharp carbonate concentrations, abrupt and wavy boundary. | 5 |
| **6** | R | 7.0–8.3 | 1.3 | Eolianite, dull orange (7.5YR 7/4), abrupt and wavy boundary. | 6 |
| **7** | Bkb | 8.3–9.3 | 1.0 | Silty clay, brown (7.5YR 4/3 dry), moderate medium columnar structure, moderately sticky, moderately plastic, common medium prominent black iron-manganese nodules, few medium-coarse irregular moderately cemented diffuse carbonate concentrations, gradual and smooth boundary. | 7 |
| | Bwb | 9.3–10.5 | 1.2 | Silty clay, brown (7.5YR 4/3 dry), moderate medium columnar structure, moderately sticky, moderately plastic, common medium prominent black iron-manganese nodules, abrupt and wavy boundary. | |
| **8** | Bkm | 10.5–10.8 | 0.3 | Calcrete, hard, gradual and smooth boundary. | 8 |
| | R | 10.8–13.8 | 3.0 | Carbonate-rich beach rock, few quartz sand seized grains, hard, many roots remnants, abundant horizontal bedding. | 9 |
| **9** | R | 13.8 + | – | Marl (not sampled). | – |

**Table 2**. Central and southern pedo-sedimentary (PS) sequences.

| PS unit | Horizon | Depth (m) | Thickness (m) | Description | Sample (Evron-#) |
|---|---|---|---|---|---|
| **1** | Bw | 0–1.0 | 1.0 | As in eastern wall. | 10 |
| **3** | Bkb | 1.0–2.3 | 1.3 | As in eastern wall. | 9 |
| **4b** | Bkb | 2.3–3.0 | 0.7 | Sandy clay loam, bright reddish-brown (5YR 5/6 dry), massive, few fine prominent black iron-manganese nodules, common-many coarse-very coarse irregular indurated sharp carbonate concentrations, gradual and smooth boundary. | 8 |
| | Bw | 3.0–4.0 | 1.0 | Sandy loam, bright reddish-brown (5YR 5/6 dry) massive, few fine prominent black iron-manganese nodules, abrupt and wavy boundary. | 7 |
| **5** | Bkb | 4.0–6.0 | 2.0 | Clay, brown (7.5YR 4/3 dry), moderate medium columnar structure, moderately sticky, moderately plastic, common slickensides, common medium prominent black iron-manganese nodules, few coarse–very coarse irregular indurated sharp carbonate concentrations, abrupt and wavy boundary. | 6 |
| | Bwb | 6.0–6.3 | 0.3 | Clay, bright brown (7.5YR 5/6 dry) massive, two grain populations: brown clay with manganese nodules and rock fragments (carbonate and chert), abrupt and wavy boundary. | 5 |
| **7** | Bkb | 6.3–7.1 | 0.8 | Clay, brown (7.5YR 4/3 dry), moderate medium columnar structure, moderately sticky, moderately plastic, common slickensides, common medium prominent black iron-manganese nodules, few coarse-very coarse irregular indurated sharp carbonate concentrations, gradual and smooth boundary. | 4 |
| | Bkb | 7.1–8.5 | 1.4 | Clay, brown (7.5YR 4/3 dry), moderate medium columnar structure, moderately sticky, moderately plastic, common slickensides, common medium prominent black iron-manganese nodules, common many coarse-very coarse irregular indurated sharp carbonate concentrations, abrupt and wavy boundary. | 3 |
| **8** | R | 8.5 + | – | As in eastern wall. | 1, 2 |

https://doi.org/10.1017/qua.2018.107 Published online by Cambridge University Press

**Table 3**. The Western pedo-sedimentary (PS) sequence.

| PS unit | Horizon | Depth (m) | Thickness (m) | Description | Sample (Evron-#) |
|---|---|---|---|---|---|
| **1** | Bw | 0–1.0 | 1.0 | As in eastern wall. | – |
| **3** | Bkb | 1.0–2.3 | 1.3 | As in eastern wall. | 100 |
| **4c** | Bkb | 2.3–5.6 | 3.3 | Clay, dark grayish-yellow (2.5 YR 5/2), massive, few fine prominent black iron-manganese nodules, common many coarse-very coarse irregular indurated sharp carbonate concentrations, gradual and smooth boundary. | 101 |
| | Bw | | | Clay, dark grayish-yellow (2.5 YR 5/2), massive, few fine prominent black iron-manganese nodules, abrupt and wavy boundary. | 102 |
| **5** | Bkb | 5.6–12.6 | 7.0 | Clay, brown (7.5YR 4/3 dry), moderate medium columnar structure, moderately sticky, moderately plastic, common slickensides, common medium prominent black iron-manganese nodules, common many coarse-very coarse irregular indurated sharp carbonate concentrations, abrupt and wavy boundary. | 103 |
| | Bkb | | | Clay, brown (7.5YR 4/3 dry), moderate medium columnar structure, moderately sticky, moderately plastic, common slickensides, common medium prominent black iron-manganese nodules, few coarse-very coarse irregular indurated sharp carbonate concentrations, abrupt and wavy boundary. | |
| | Bwb | | | Silty clay, bright brown (7.5YR 5/6 dry) massive, two grain populations: brown clay with manganese nodules and rock fragments (carbonate and chert); abrupt and wavy boundary. | 104 |
| **7** | Bkb | | | Clay, brown (7.5YR 4/3 dry), moderate medium columnar structure, moderately sticky, moderately plastic, common slickensides, common medium prominent black iron-manganese nodules, few coarse-very coarse irregular indurated sharp carbonate concentrations, gradual and smooth boundary. | 105–107 |
| **8** | R | 12.6+ | – | As in eastern wall. | – |

reverse) is that at least two samples, one demagnetized thermally and another with AF, show similar and identical unambiguous results. Horizons that do not meet the above criterion but have at least one sample with clear polarity interpretation are marked with a question mark (i.e., N? or R+?). Figure 4 shows demagnetization results from two horizons meeting the above reliability criterion. The upper panel shows a univectorial normal polarity magnetization with north-northeast declinations and downward inclinations. The lower panel shows a primary reversed polarity vector overprinted by secondary normal polarity viscous magnetization. Out of 26 horizons, 11 had reliable polarity interpretations, 14 had questionable interpretations, and one did not provide any successful interpretation (Fig. 3 and 4; Supplementary Figures 2–6; Supplementary Tables 1–5). The horizon that failed is a fluvial horizon in Unit 5 that contained a major component of small flint items (Fig. 5b).

### *Southern sequence (Fig. 5a)*

The southern landfill wall provided the most complete sedimentological sequence to be sampled for paleomagnetic stratigraphy. Three reversals were identified in this sequence —one in Unit 4b and two in Unit 7. Assuming that the age of Unit 3 is a few thousand years at the most, based on previous works (Porat and Ronen, 2002; Ron et al., 2003), the Brunhes–Matuyama (BM) boundary (0.77 Ma) is located in Unit 4b. The normal horizon bracketed by reversed horizons in Unit 7 is most likely the Jaramillo normal subchron (1.076–1.008 Ma). Two additional possible interpretations for the normal horizon are the Cobb Mtn (1.221–1.189 Ma) and Olduvai (1.934–1.787 Ma). The Cobb Mtn is too short to enable magnetic recording in these types of sediments, and therefore this interpretation is unlikely. The Olduvai interpretation demands that either the Jaramillo subchron is not represented in the sequence, or that the sampling resolution is insufficient for recovering the Jaramillo. Taken altogether, we conclude the base of the southern section within Unit 7 must be older than the Jaramillo, i.e., older than 1.076 Ma.

### *Central sequence (Fig. 5b)*

The Central sequence comprises a segment of Units 5 with a fluvial wedge, rich with small flint items, that thickens northward. The polarity of this fluvial unit could not be determined because one sample (EQP-29, Supplementary Material) showed a primary reverse magnetization overprinted by a secondary normal magnetization, but a neighboring sample (EQP-30, Supplementary Material) showed a contradicting result of a primary normal magnetization. This unit separates an overlying normal polarity horizon from an underlying reversed horizon. Thus, even if the polarity of the unit could not be determined, its age is likely to be near the BM boundary.

### *Trench T2 (Fig. 5d)*

The polarity of the three horizons in trench T2 is normal. The stratigraphic correlation between the upper fine-grained

https://doi.org/10.1017/qua.2018.107 Published online by Cambridge University Press

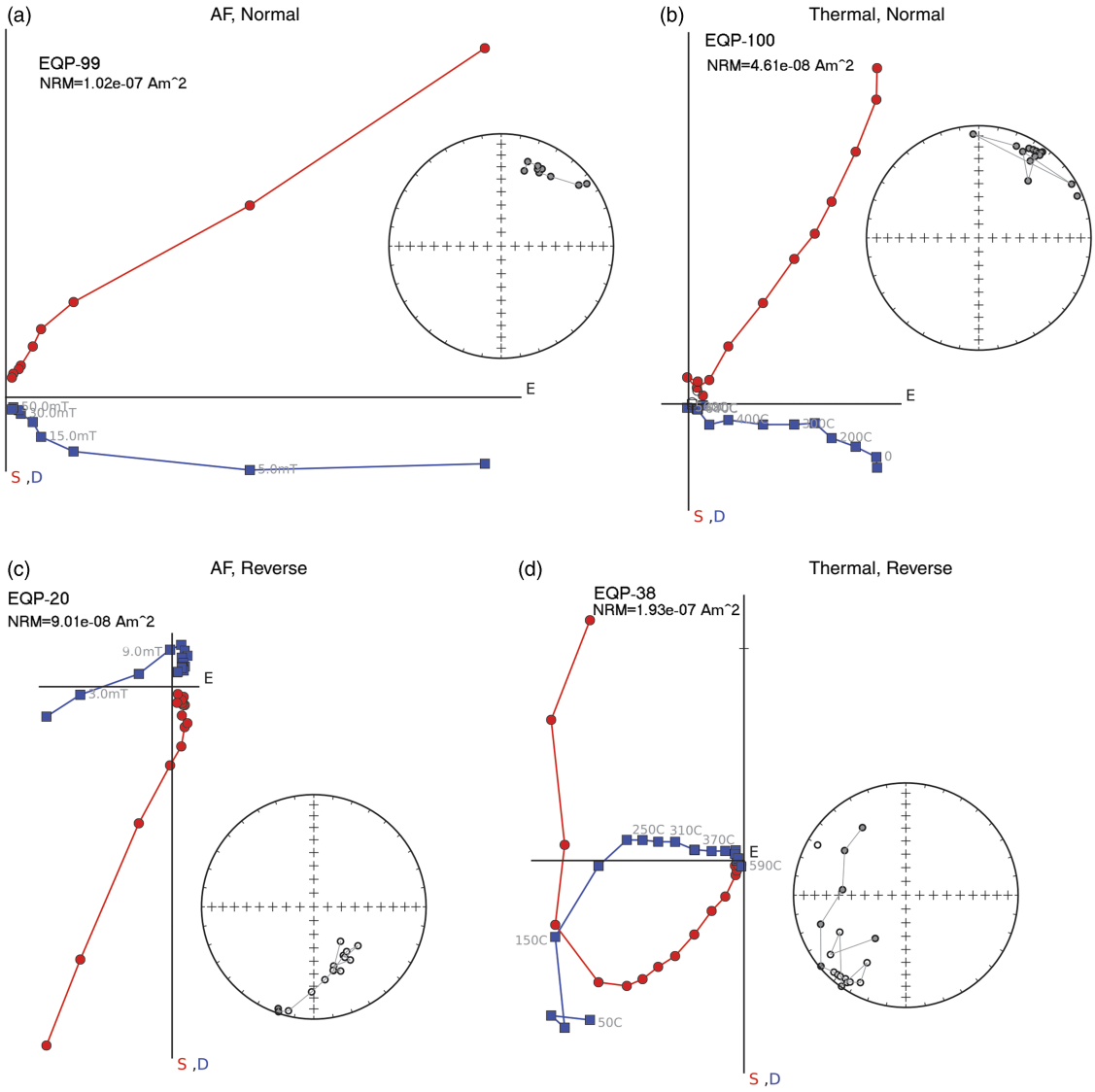


**Figure 4.** (a and c) Representative results of alternating field and (b and d) thermal demagnetizations shown as Zijderveld plots (Zijderveld, 1967) and equal area projection. (a) and (b) display two samples from the same horizon showing univectorial normal polarity magnetization. (c) and (d) from the same horizon show primary reverse magnetization, where (d) is overprinted by a secondary normal magnetization. Blue (red) squares (circles) are projections of the paleomagnetic direction on the horizontal (vertical) planes. (For interpretation of the references to color in this figure legend, the reader is referred to the web version of this article.)

alluvial unit in the trench (normal polarity) and the lowermost horizon in the Central section (Fig 5b., reverse polarity) is not clear, owing to the cut-and-fill morphology. Thus, a clear magnetostratigraphic affiliation of the trench cannot be firmly determined.

### *Northern sequence (Fig. 5c)*

The stratigraphy of the Northern sequence comprises Units 3–7. Here, no clear reversals where found in Units 4–5, but a questionable reversed horizon overlying a normal horizon was found in the transition between Unit 5 and Unit 7. We suggest that this reverse horizon is in the same stratigraphic position as the reverse horizon in the Central sequence (Fig. 5b).

## Dating by cosmogenic isotope burial ages

$^{10}$Be concentrations range between $20.97 \pm 0.60 \times 10^4$ atoms/g quartz and $26.42 \pm 0.76 \times 10^4$ atoms/g quartz. $^{26}$Al concentrations follow a similar pattern to that of $^{10}$Be and they range between $58.76 \pm 3.5 \times 10^4$ atoms/g quartz and $87.17 \pm 4.5 \times 10^4$ atoms/g quartz (Table 4). $^{26}$Al/$^{10}$Be ratios range between $2.80 \pm 0.18$ and $3.30 \pm 0.20$. Concentrations and $^{26}$Al/$^{10}$Be in the two lower samples (EQ-1 and EQ-2) are similar. Concentrations and $^{26}$Al/$^{10}$Be in the upper sample (EQ-3) are higher.

When assuming an initial $^{26}$Al/$^{10}$Be ratio of 6.8 (the production rate ratio) these ratios imply ages of $1.69 \pm 0.21$ Ma (EQ-1), $1.60 \pm 0.20$ Ma (EQ-2), and $1.36 \pm 0.18$ Ma (EQ-3 and Fig. 6). However, Davis et al. (2012) showed that Nilotic sands along the eastern coast of the Mediterranean are

https://doi.org/10.1017/qua.2018.107 Published online by Cambridge University Press

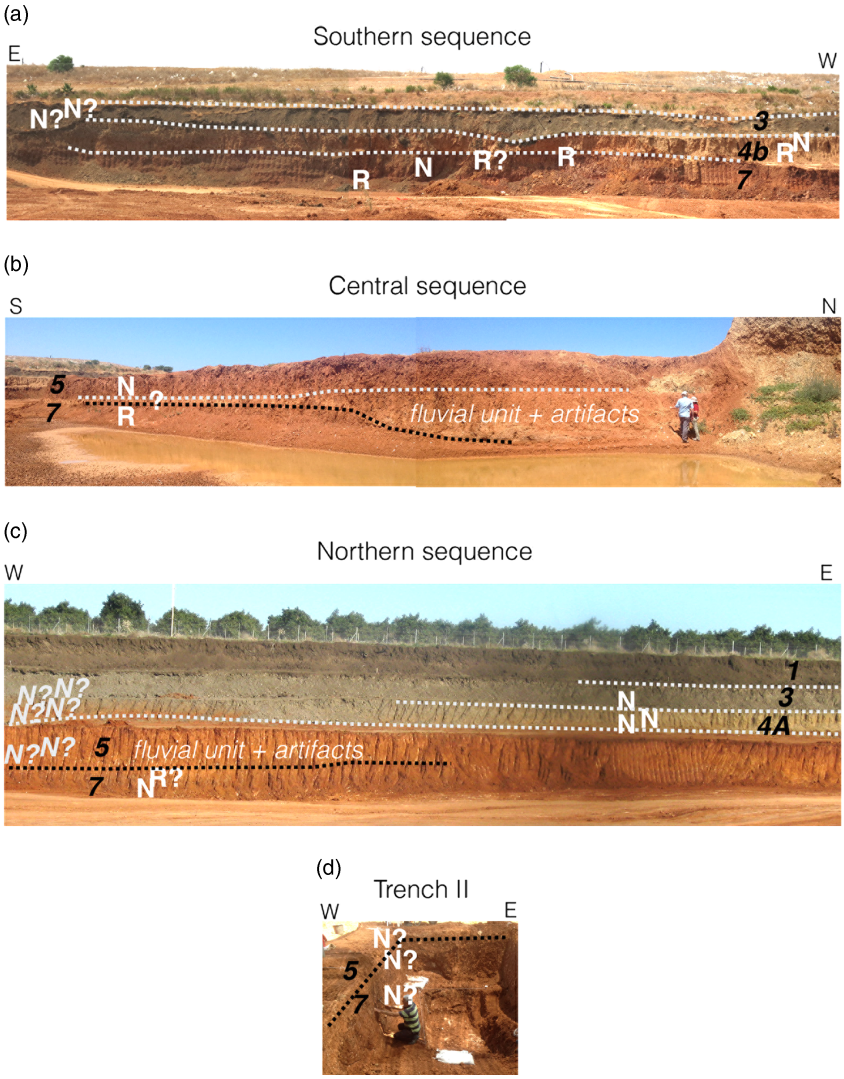


**Figure 5.** Paleomagnetic stratigraphy. White dashed lines show main stratigraphic boundaries; black dashed line shows erosional disconformity in Unit 5; numbers correspond to units within the pedo-sedimentary sequence (see text). Paleomagnetic interpretations are marked with N (normal) and R (reverse). A question mark is added when interpretation is not supported by both AF and thermal demagentizations.

typically deposited with $^{26}Al/^{10}Be$ ratios that range between $4.46 \pm 0.28$ and $4.92 \pm 0.35$ ($n = 4$), corresponding to an average apparent burial age $0.69 \pm 0.085$ ka. This depressed ratio, relative to the production rate ratio, results from a complex exposure-burial history of the sands while being transported along the Nile, its delta, and then along the eastern Mediterranean shore by long-shore currents. Thus, corrected ages can be obtained by subtracting the apparent initial age from the simple burial ages. This subtraction yields corrected ages of $0.99 \pm 0.1$ Ma (EQ-1), $0.90 \pm 0.13$ Ma (EQ-2), and $0.66 \pm 0.11$ Ma for the upper sample (EQ-3; Table 5). It is important to clarify here, however, that, although the corrected cosmogenic burial ages are the most probable ones, within analytical error, the age of EQ3 may be as old as 0.77 Ma (nearly at the BM transition). Furthermore, it is theoretically possible that for a specific sample, the initial ratio at the time of burial may be over- or underestimated, invalidating the corrected age.

## The archaeological finds

### *The lithic assemblage*

The lithic assemblage from 'Evron Landfill is small, comprising a total of 236 items (Table 6). Only 31 artifacts were retrieved from clear excavation contexts, while the rest were collected from the surrounding area, enabling their ascription to a sedimentological unit, but with no clear stratigraphic correlation to the finds in trench T2. Most prominent are several large core tools: two hand axes, three spheroids, and three choppers (Fig. 7), comprising a third of all tools in the assemblage (Table 7).

Flint is the dominant raw material used;, however, all three spheroids and the hammerstone found in the assemblage are made of hard limestone. Two additional limestone pebbles that display several removal scars, as well as several limestone flakes, might represent broken or discarded hammerstones.

https://doi.org/10.1017/qua.2018.107 Published online by Cambridge University Press

**Table 4**. Field and cosmogenic data for 'Evron Landfill samples. Be spike concentration = –1414 ppm. Uncertainties in concentrations include spike uncertainty added in quadrature. $^{10}Be/^{9}Be$ are blank corrected and normalized to NIST SRM-4325 = $2.790 \times 10^{-11}$. Presented values are corrected for procedural blank. $^{26}Al/^{27}Al$ ratios are blank corrected and normalized to $Al_2O_3$ SD = $7.401 \times 10^{-12}$. Presented values are corrected for procedural blank.

| Sample (EQ-#) | Description | Burial depth (m) | Sample mass (g) | Be spike (g) | $^{10}Be/^{9}Be^{\S}$ ($\times 10^{-14}$) | $^{10}Be$ ($\times 10^{4}$ atoms/g) | [Al] ($10^{18}$ atoms/g) | $^{26}Al/^{27}Al^{\#}$ ($\times 10^{-14}$) | $^{26}Al$ ($\times 10^{4}$ atoms/g) | $^{26}Al/^{10}Be$ |
|---|---|---|---|---|---|---|---|---|---|---|
| **1** | Aeolionite – massive | 12.9 | 25.067 | 0.181 | $30.97 \pm 0.6$ | $20.97 \pm 0.58$ | 1.44 | $40.90 \pm 1.82$ | $58.76 \pm 3.5$ | $2.80 \pm 0.18$ |
| **2** | Aeolionite – layered | 12.5 | 24.971 | 0.181 | $31.13 \pm 0.52$ | $21.16 \pm 0.55$ | 2.12 | $29.34 \pm 1.28$ | $62.26 \pm 3.7$ | $2.94 \pm 0.19$ |
| **3** | Massive red clay | 10.0 | 26.661 | 0.182 | $41.28 \pm 0.85$ | $26.42 \pm 0.76$ | 1.52 | $57.22 \pm 1.91$ | $87.17 \pm 4.5$ | $3.30 \pm 0.20$ |

Cores comprise ca. 23% of the assemblage (Table 6). Polyhedral cores are the most common (26 of 54 cores), demonstrating the utilization of multiple faces for flake production (Fig. 8.1 and 8.3). Prismatic cores are relatively few (n = 7), displaying a volumetric concept for the production of elongated flakes (Fig. 8.2). Tested nodules (n = 21) comprise the rest of this category. Many of the cores (n = 34; ca. 64%) are small, with metric values measuring less than 3 cm. While many are very exhausted, some of these cores still retain cortex and demonstrate that the initial size of the nodules was small. Accordingly, these nodules were designated for the intentional production of small flakes (Fig. 8). These somewhat resemble the industry described by Chazan (2013) in the Evron Quarry assemblage. A similar industry was also described at the site of Bizat Ruhama (Zaidner et al., 2003; Zaidner, 2014).

Tools comprise ca. 10% of the assemblage, including both retouched and core tools. Flakes and primary flakes are the most common blank types, representing 25% and ca. 17% of this category, respectively (Table 7). Most frequent tool types are side scrapers (n = 5) and perforators (n = 5), each comprise ca. 21% of this category. There is one multiple tool, displaying a combination of truncation with limited scraper retouch. Other retouched tools include end scrapers, denticulates, and retouched flakes (Table 7).

Choppers vary in size, presenting a range of 4–7.8 cm in length, 4.3–6.9 cm in width, and 5.1–7.6 cm in thickness. Hand axes are relatively coarse, with an average length of 12.4 cm and an average width of 6.7 cm (Fig. 7). Both present deep scars, indicating the use of hard-hammer percussion for their production. These were made of two distinct raw material types: the first (Fig. 7:1) was made of a whitish-gray

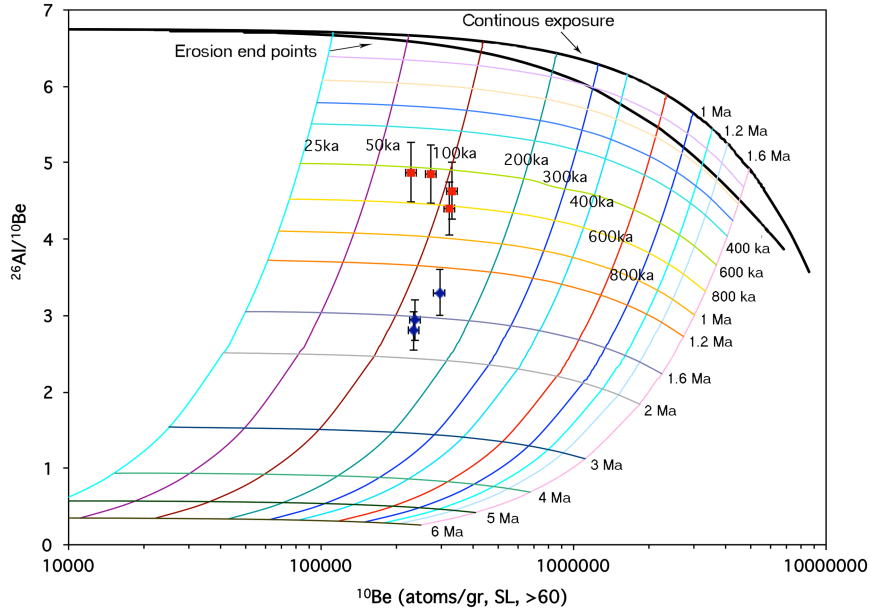


**Figure 6.** $^{10}Be$ concentrations and $^{26}Al/^{10}Be$ ratios of samples from 'Evron Landfill (blue markers). Modern sand samples (Davis et al., 2012) are indicated with red markers. Initial exposure periods are indicated with plain numbers. Burial isochrones are indicated by bold numbers. (For interpretation of the references to color in this figure legend, the reader is referred to the web version of this article.)

https://doi.org/10.1017/qua.2018.107 Published online by Cambridge University Press

**Table 5**. Burial ages for 'Evron Landfill samples. Scaling factors for spallation were calculated using Lal-Stone (2000). Sea-level high-latitude production rates due to spallation for $^{10}$Be and $^{26}$Al in quartz are 4.5 ± 0.52 and 30.0 ± 3.5 atoms/g/yr, respectively (Balco et al., 2008). Muon production rates and altitude scaling are based on Granger and Muzikar (2001). Half-lives for $^{10}$Be and $^{26}$Al are 1.39 ± 0.01 and 0.705 ± 0.02 Ma, respectively (Chmeleff et al., 2010; Korschinek et al., 2010; Nishiizumi, 2004). Elevation = 30 m asl; latitude = 33°N. Corrected age is calculated by subtracting the average apparent burial age of modern coastal-plain sands from the simple burial age of each sample. The apparent average burial age of modern sands is calculated from the $^{26}$Al/$^{10}$Be ratio measured in four modern sand samples (Davis et al., 2012).

| Sample (EQ-#) | Simple burial age (Ma) | Corrected burial age (Ma) |
|---|---|---|
| **1** | 1.69 ± 0.21 | 1.1 ± 0.2 |
| **2** | 1.60 ± 0.20 | 1.0 ± 0.2 |
| **3** | 1.36 ± 0.18 | 0.77 ± 0.2 |

coarse-grained flint; the second, oval in shape (Fig. 7:2), was made of a translucent quarzitic raw material.

## *The Faunal assemblage*

Seven faunal skeletal elements were recovered from 'Evron Landfill, representing three different taxa:

(1) A medium-sized artiodactyl cf. *Dama* sp., represented by a humerus shaft (Fig. 9a), with minimal shaft width above the distal end of 26.18 mm. Remains of *Cervus elaphus* and of a smaller cervid cf. *Capreolus*, were identified from the earlier Evron Quarry excavations (Tchernov et al., 1994), but no remains of fallow deer. At the LP site of Gesher Benot Ya'akov, remains of *Dama* sp. comprise the majority of identified fauna and fall within the size range documented for modern female *Dama mesopotamica* (Rabinovich et al., 2011).

(2) An extinct equid, *Equus.* cf. *tabeti*, represented by an upper right first ($M^1$) or second molar ($M^2$; Fig. 9b) using dental criteria developed by Eisenmann et al. (1988) and papers on the dental biometry and morphology of Levantine Paleolithic equids (e.g. Davis 1980; Eisenmann 1986, 1992, 2012a, 2012b). The 'Evron Landfill molar has a small protocone with a small caballine fold present, while the enamel of the fossettes is moderately plicated (Fig. 9b). These morphological features are also visible in upper molars from 'Ubeidiya and Gesher Benot Ya'akov that have also been assigned to *E.* cf. *tabeti* (Eisenmann, 1986, 2012a). Dimensions (in mm) of the 'Evron Landfill tooth are: occlusal length = 25.28; occlusal breadth = 26.14; basal length = 21.33; basal breadth = 24.36; and protocone length = 11.44. Based on occlusal size and protocone length, as illustrated in Figure 10, the 'Evron Landfill specimen falls within the upper size range *E. tabeti* $M^1$/$M^2$'s from Aïn Hanech (Algeria) and close to a specimen from Gesher Benot Ya'akov (and also Bizat Ruhama; fig. 9 in Yeshurun et al., 2011), while it differs slightly from a specimen from 'Ubeidiya, which has a shorter protocone but larger occlusal diameter. Though no equid remains were recovered during the initial investigations at Evron Quarry (Tchernov et al., 1994), three of the four equid cheek teeth from surface collections at the LP site of Oumm Zinat, located some 500 m east of Kibbutz Evron (Horwitz and Tchernov, 1989), resemble those of *E.* cf. *tabeti* (Eisenmann, 2012b), indicating continuity of this taxon during the LP in the Evron find locality.

(3) A large bovid identified as *Bos cf. primigenius* is represented by a lower left second molar ($M_2$, still erupting; Fig. 9c and d) as well as two unconjoined lobes (anterior and middle) of a lower left third molar ($M_3$) from an older individual. Following criteria given in Slott-Muller (1990), both molars from the new excavations at 'Evron Landfill conform to morphological features considered typical of *Bos* rather than *Bison*. The central buccal column of the $M_2$ is straight and begins at the cemento-enamel junction, with no apparent thickening at the cervix; the crown base, though damaged, appears to be straight and not "swollen" as in *Bison*. The tooth is quite large (Supplementary Table 6) and moderately hyposodont; the enamel is thick and the roots are patent. A lower right $M_1$ from the excavations at Evron Quarry was also attributed to *Bos* cf. *primigenius* (Tchernov et al., 1994) and closely resembles the finds from the Landfill site. *Bos* cf. *primigenius* has been identified in the middle Pleistocene quarry of Qadib el-Ban located within the Latamne Formation in Lebanon, where it occurs together with *Bison priscus* (Guérin et al., 1993), while at the roughly contemporaneous site of Gesher Benot Ya'akov, an unspecified form of *Bos* was recognized

**Table 6**. General breakdown of the lithic assemblage from 'Evron Landfill.

| Category | n | % |
|---|---|---|
| **Flakes** | 45 | 56.25 |
| **Primary flakes (retaining more than 50% cortex)** | 11 | 13.75 |
| **Core trimming elements (CTEs)** | 20 | 25.00 |
| **Naturally backed items (NBKs)** | 3 | 3.75 |
| **Total** | 80 | 100.00 |
| | | |
| **Chips** | 27 | 40.91 |
| **Chunks** | 39 | 59.09 |
| **Total** | 66 | 100.00 |
| | | |
| **Debris** | 66 | 27.97 |
| **Debitage** | 80 | 33.90 |
| **Tools** | 24 | 10.17 |
| **Cores** | 54 | 22.88 |
| **Hammerstone** | 1 | 0.42 |
| **Limestone artifacts** | 11 | 4.66 |
| **Total** | 236 | 100.00 |

https://doi.org/10.1017/qua.2018.107 Published online by Cambridge University Press

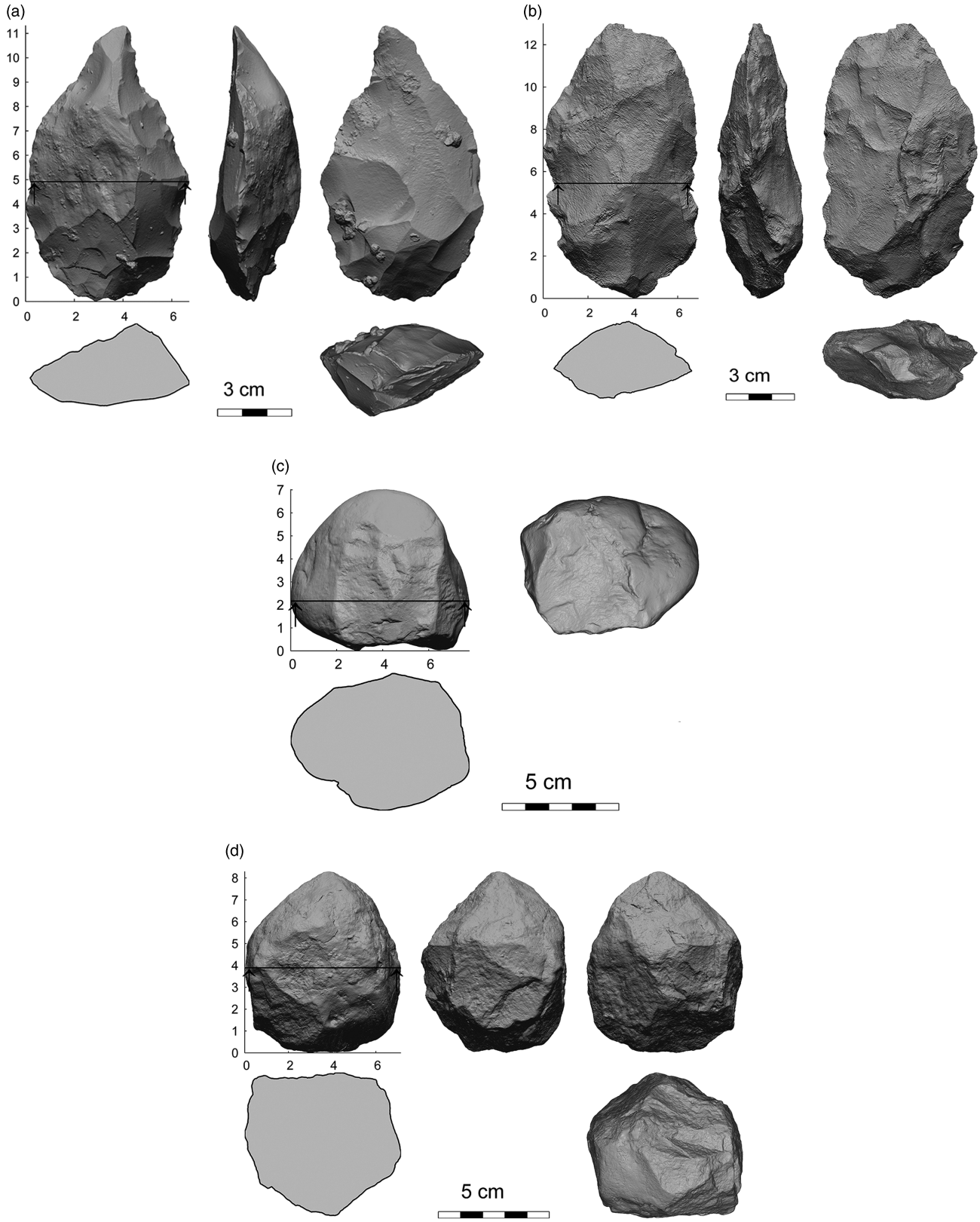


**Figure 7.** Large tools from the 'Evron Landfill assemblage: (a and b) handaxes, (c) a chopper, and (d) a spheroid (3-d scans by Argita Levanon, courtesy of the Israel Antiquities Authority).

(Hooijer, 1959; Geraads and Tchernov, 1983; Martínez-Navarro and Rabinovich, 2011; Rabinovich et al., 2011). *Bos primigenius* is absent in the earlier site of 'Ubeidiya (Bar-Yosef and Belmaker, 2011; Martínez-Navarro et al., 2012) such that finds from the 'Evron site complex, Latamne and possibly also Gesher Benot

https://doi.org/10.1017/qua.2018.107 Published online by Cambridge University Press

**Table 7**. Tools and blank types frequencies.

| Tool type | | Flakes | Primary flakes | Core trimming elements | Naturally backed items | Flint nodules | Limestone nodules | Not identified | Total n | Total % |
|---|---|---|---|---|---|---|---|---|---|---|
| **Hand axes** | | | | | | 2 | | | 2 | 8.33 |
| **Choppers** | | | | | | 3 | | | 3 | 12.50 |
| **Spheroids** | | | | | | | 3 | | 3 | 12.50 |
| **Perforators** | | 2 | 1 | | | | | 2 | 5 | 20.83 |
| **Sidescrapers** | | 2 | 1 | | 1 | 1 | | | 5 | 20.83 |
| **End scrapers** | | | 1 | 1 | | | | | 2 | 8.33 |
| **Denticulates** | | 1 | | | | | | | 1 | 4.17 |
| **Retouched flakes** | | | 1 | | 1 | | | | 2 | 8.33 |
| **Multiple tools** | | 1 | | | | | | | 1 | 4.17 |
| **Total** | n | 6 | 4 | 1 | 2 | 6 | 3 | 2 | 24 | 100.00 |
| | % | 25.00 | 16.67 | 4.17 | 8.33 | 25.00 | 12.50 | 8.33 | 100.00 | |

Ya'akov may represent the earliest remains of this species in the Levant. From ca. 0.5 Ma onwards, *Bos primigenius* is well-established in the Levant and occurs in numerous sites (e.g. Horwitz and Monchot, 2007; Stiner et al., 2009; Reynaud Savioz, 2011; Yeshurun et al., 2011; Rabinovich et al., 2012).

(4) Additional faunal remains from 'Evron Landfill that could not be identified to taxon are: a fragment of mammalian tooth enamel; six long-bone shaft fragments from a large-sized mammal (not Proboscidean); proximal metapodial fragment of a large-sized mammal.

In sum, all taxa identified in the 'Evron Landfill assemblage occur in other Levantine early mid-Pleistocene sites such as Latamne, Bizat Ruhama, and Gesher Benot Ya'akov.

## DISCUSSION

### 'Evron Landfill and other LP sites in the Southern Levant

The estimated age of 'Evron Landfill is based here on paleomagnetic stratigraphy anchored by cosmogenic isotope burial ages. The results indicate that hominin activity in this locality took place near the BM transition, ca. 0.77 Ma.

Cosmogenic isotope dating anchors the paleomagnetic stratigraphy of Unit 5. Since this unit is not represented in the Southern sequence, its correlation to Unit 4b, in which the BM transition was identified, is unknown. In addition, no clear magnetostratigraphic affiliation could be achieved from the samples of Unit 5 in the Western and Northern sequences. Still, its stratigraphic position in both described sequences indicates that the age of Unit 5 should be near the BM transition, ~0.77 Ma. The corrected cosmogenic age of the bottom part of Unit 5, just above its contact with Unit 7 in Trench 2 (Fig. 3 and 5; Table 5) is $0.66 \pm 0.11$ Ma. This result supports the magnetostratigraphic observation and provides a minimum age for the accumulation of Paleolithic finds, which originated from the contact between Units 5 and 7. A maximum age is provided by paleomagnetic stratigraphy, indicating that the base of Unit 7 is older than 1.076 Ma. The stratigraphic position of the archaeological finds, however, located in the contact between sedimentological Units 5 and 7, suggests that hominin activity took place in the early depositional phases of Unit 5, when the top of Unit 7 was exposed on the surface. Following this hypothesis, the time of deposition of the archaeological finds should be closer to the age of Unit 5, i.e., ~0.77 Ma.

These ages fit well with the faunal composition, which demonstrates similarities to other, early middle-Pleistocene sites such as Latamne, with an estimated age of 0.7–0.5 Ma (Guérin et al., 1993; Sanlaville et al., 1993) and Evron Quarry and Gesher Benot Ya'akov, dated between 1.0–0.77 Ma (e.g., Gilead and Ronen, 1977; Goren-Inbar et al., 2011; Porat and Ronen, 2002; Ron et al., 2003; Rink and Schwartz, 2005; Rabinovich et al., 2011; Yeshurun et al., 2011).

All the faunal taxa identified in 'Evron Landfill were also found, either together or singly, in other roughly contemporaneous early mid-Pleistocene Levantine sites such as of Latamne, Evron Quarry, and Gesher Benot Ya'akov. In terms of biochronology the site is then constrained between the early Pleistocene site of 'Ubeidiya which lacks three of the taxa (i.e., *E. tabeti, Dama* sp., *Bos* cf. *primigenius*) and numerous late LP sites in the region (Revadim, Holon, Qesem, Hummal, Nadayouieh.) which lack *E. tabeti*. Though chronological inferences based on isolated finds are problematic, there is a high degree of biochronological accord when all taxa are examined.

The lithic assemblage of 'Evron Landfill presents affinities mostly with Early Acheulian industries: hand axes are relatively coarse, displaying large, deep scars indicating the use of a hard-hammer percussion through all production stages, and a distinct component of a small-flake (>3 cm) industry is present. Still, this is a small collection and by itself is insufficient for establishing a clear cultural affiliation. Considering the suggested age range obtained through paleomagnetic

https://doi.org/10.1017/qua.2018.107 Published online by Cambridge University Press

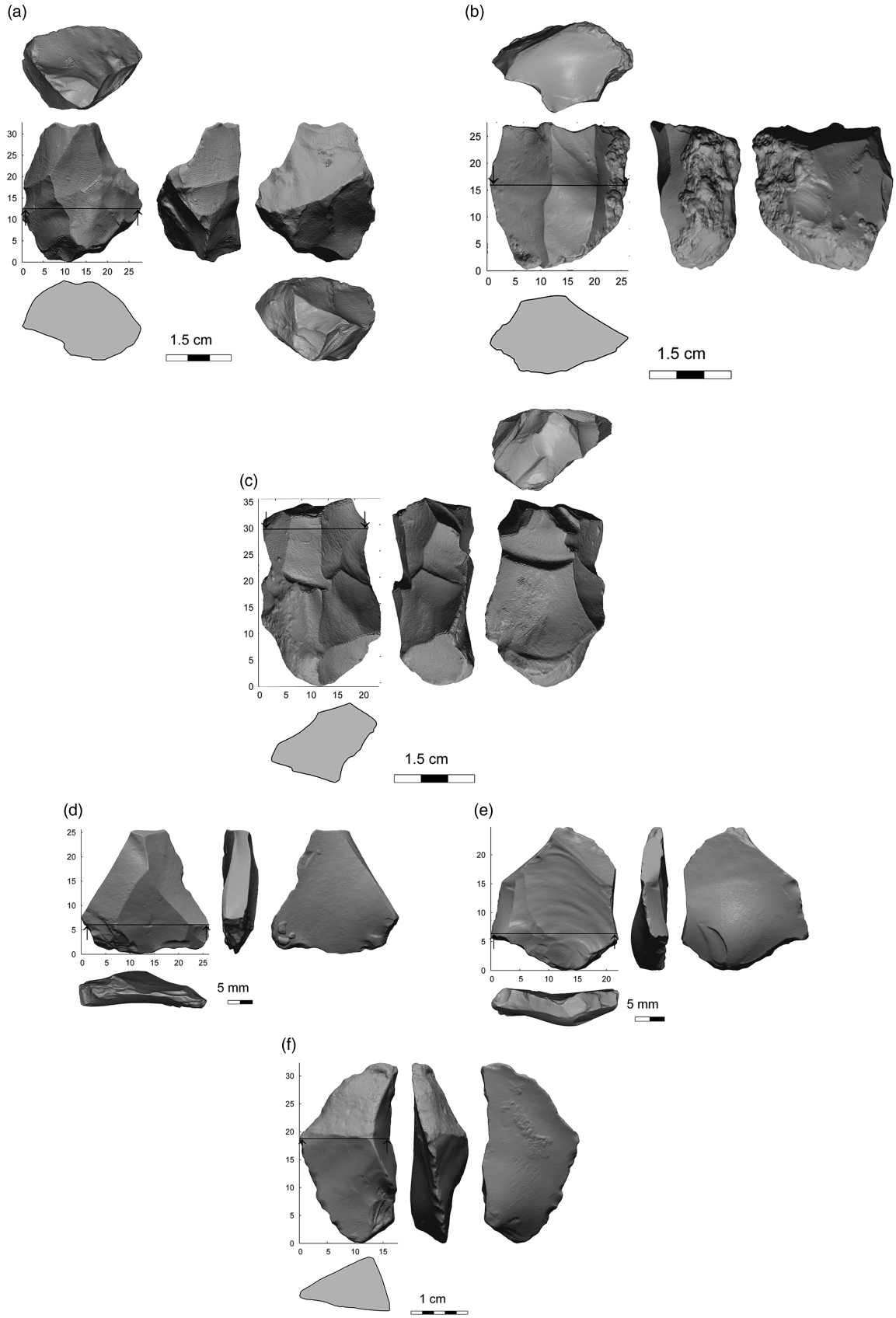


**Figure 8.** The small flakes industry component in the 'Evron Landfill assemblage: (a–c) cores, (d and e) "Levallois-like" flakes, and (f) CTE (3-d scans by Argita Levanon, courtesy of the Israel Antiquities Authority).

https://doi.org/10.1017/qua.2018.107 Published online by Cambridge University Press

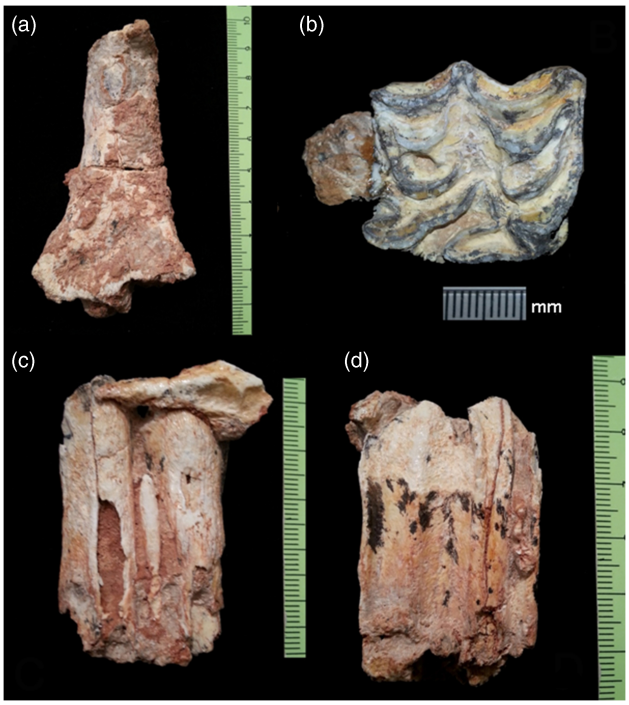


**Figure 9.** (color online) Faunal remains from 'Evron Landfill. (a) *Dama* sp. Right distal humerus shaft, anterior aspect. (b) *Equus* cf. *tabeti* upper first or second molar, occlusal aspect. (c) *Bos* sp. lower second molar, lingual aspect. (d) *Bos* sp. lower second molar, buccal aspect.

stratigraphy and cosmogenic isotope burial age, however, and the biochronological data retrieved from the faunal assemblage, it is suggested that the material culture and faunal assemblage of 'Evron Landfill are sufficiently indicative to be attributed to the Early Acheulian. The geographic proximity between 'Evron Landfill and Evron Quarry, as well as the correlation between sedimentological units and resemblance lines observed in lithic and faunal composition between both assemblages, might indicate a connection between these two localities, possibly representing a single site.

## The depositional environments of 'Evron Landfill

Most of the units at the site are part of the 'Evron Member of the Quaternary Hefer Formation, which are comprised of alternating red sandy loam soils (Hamra) and eolianites (Gvirtzman et al., 1984; Sivan, 1995; Sivan et al., 1999). Lithostratigraphic and pedologic studies in Evron Quarry, located only 300 m south to the study site, have defined eight pedo-sedimentary units in the 8.5-m-thick section exposed at that site, and provide us with a geological and environmental reference (Table 8; Ronen and Amiel, 1974; Ronen 1991).

The results of the pedo-sedimentary investigation of 'Evron Landfill reveal a ~14-m-thick complex sequence in which eight units were defined. The entire sequence can be divided into two broad depositional environments: the lower units of the sequence (Units 4–8) demonstrate dynamic coastal environments, whereas the upper units (Units 1–3) represent a more inland environment, not necessarily coastal.

The base of the landfill (Unit 9) is characterized by yellow marls, which were not sampled in this study. This unit correlates to Unit 8 in the study of Ronen and Amiel (1974), described as Miocene marl. According to Issar and Kafri (1969), these marls are of early Miocene age (23–16 Ma).

Unconformably overlaying the marls is a prominent ~3-m-thick carbonate-rich beach rock (Unit 8). Its composition and inclination indicate that it formed in an ancient shore environment. This beach rock correlates to Unit 7 in Ronen and Amiel (1974), which was defined as 2–4 m thick eolianite. The facies change probably represents inland transition from beach rock to eolianite. Based on Sivan et al. (1999), this unit is ascribed to the Kurdane Formation (Kafri and Ecker, 1964) and is equivalent to the Pliocene Pleshet

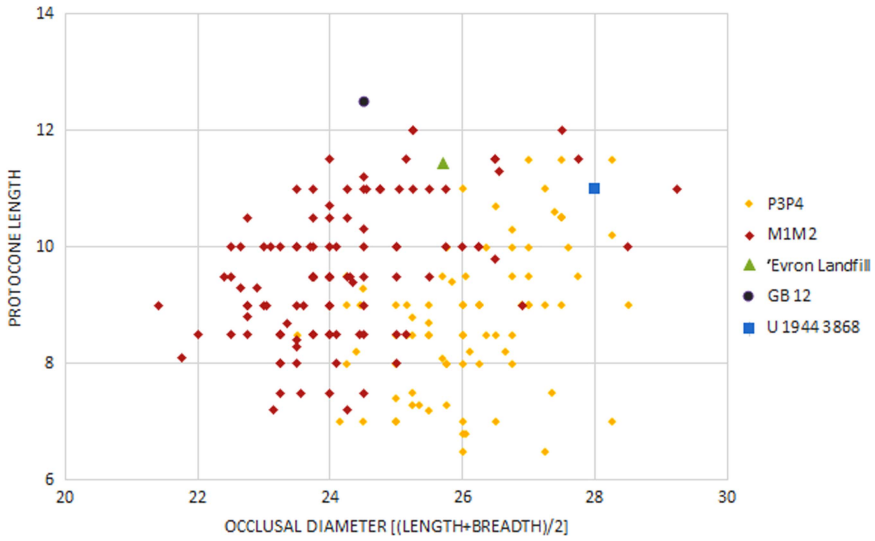


**Figure 10.** (color online) Metric values of the *Equus* cf. *tabeti* molar from 'Evron Landfill, compared to equid molars from Gesher Benot Ya'akov (GB12) and from 'Ubeidiya (U 1944). P3P4 = third/fourth premolar; M1M2 = first/second molar.

https://doi.org/10.1017/qua.2018.107 Published online by Cambridge University Press

Formation (Gvirtzman, 1970; Buchbinder, 1975). Sivan et al. (1999) generated an isopach map of the Kurdani Formation in the region and concluded that the shoreline was then approximately 1 km west of our study site.

The age of the Kurdane Formation is inconclusive: it has been assigned to the Miocene (Kafri and Ecker, 1964), Pliocene (Zilberman, 1991), or Pliocene–Pleistocene (Gvirtzman, 1970; Buchbinder, 1975). Corals found within this formation (Sivan, 1996) imply some correlation with units that are attributed to the "Calabrian" (1.8 – 0.78 Ma) or lower Pleistocene (Reiss and Issar, 1961). In 'Evron Landfill, the age of the Kurdane Formation based on cosmogenic isotopes, ranges between $0.99 \pm 0.1$ Ma (EQ-1) and $0.9 \pm 0.13$ Ma (EQ-2). These ages correlate well with the paleomagnetic results, indicating that this unit should be older than the Jaramillo subchron, i.e., older than 1.076 Ma. Thus, we provide a more accurate age estimation for the formation of this unit.

The beach rock itself exhibits signs of pedogenesis (roots remnants), it is capped by a thick calcrete, and its upper boundary shows signs of erosion. These observations point to a long interval of subaerial exposure (and another unconformity), subsequent to the formation of the beach rock and prior the deposition of the overlying Unit 7.

Unit 7 is composed of brown sticky clay to silty clay, rich with black iron-manganese nodules. It correlates to Units 5 and 6 defined at Evron Quarry (Ronen and Amiel 1974). In places, a well-developed calcic horizon appears at the upper part of the unit. The PSD of this unit is bimodal, with a dominant clay-silt mode and a second mode at the sand fraction. Most of the sediments are fine-grained and probably originated from the drainage system to the east; the minor addition of coarse grains (sand) can originate from the underlying eolianite or from the nearby coastal sediments. The appearance of a calcic horizon at the top of the unit indicates subaerial exposure for a relatively long time period. The fine-grained sediments that dominate the deposits and the widespread appearance of iron-manganese nodules indicate redux conditions, pointing to a marsh-like environment (i.e., wetland), typical adjacent to eolianite ridges found elsewhere along the coastal plain of Israel (e.g., Sivan et al., 1999, 2001).

**Table 8**. Correlation table of the pedo-sedimentary units exposed in 'Evron Landfill and Evron Quarry.

| 'Evron Landfill (this study) | Evron Quarry (Ronen and Amiel, 1974) |
|---|---|
| **1** | 1 and 2 |
| **2** | – |
| **3** | 1 and 2 |
| **4** | 3 |
| **5** | 5 and 6 |
| **6** | – |
| **7** | 5 and 6 |
| **8** | 7 |
| **9** | 8 |

Unit 6 is a 1.3-m-thick eolianite, exposed only at the eastern wall of the landfill, and was not documented in previous studies. It dips to the west and is abruptly (horizontally) cut by Unit 5. Unit 6 was deposited in a coastal environment with a direct linkage to the seashore; its clear erosion towards the west resembles a sea-cliff morphology.

Unit 5, cutting both Units 6 and 7, is comprised of clay sediments similar to Unit 7 with alternating fluvial layers/lenses rich with sand grains. It correlates with Units 5 and 6 described by Ronen and Amiel (1974). The fluvial layers within this unit are composed of the nearby bedrock (mostly carbonate). Unit 5 represents varying environmental conditions, alternating both spatially and temporally between marsh and streams.

Unit 4 uncomfortably overlies Units 7, 6, and 5. It changes laterally, alternating from reddish-brown clay to dark-grayish yellow clay and to bright reddish-brown sandy loam to sandy clay loam, and is therefore probably not a chronostratigraphic unit. Due to these changes, it is hard to correlate Unit 4 to previous studies. However, it seems that at least the red clay facies should be correlated with Unit 3 described by Ronen and Amiel (1974). This unit represents spatially and temporally alternating environments, ranging from marsh to coastal environment with a direct linkage to the shore.

Units 1–3 are inland units, correlating with Ronen and Amiel's Units 1–2 (Ronen and Amiel, 1974). These units consist of silty clay to clay sediments that represent the alluvial fill of the region, originating from the mountains to the east. The well-developed calcic horizons that appear at the boundaries of these units suggests three stages of alluvial fill divided by non-depositional or erosional periods.

The stratigraphic position of the archaeological finds, alongside with the field observations mentioned above, indicate that hominin activity at 'Evron Landfill took place on top of Unit 7, when it was subaerially exposed. This could have occurred after the coastline retreat and during the early stages of deposition of Unit 5. The presence of small flint artifacts and fragments (<3 cm) within the fluvial lenses of Unit 5 is interpreted as a secondary deposition caused by this unit cutting through the archaeological horizon. Thus, the hominin activity in 'Evron Landfill is associated with a marsh environment.

In the scenario in which hominin activity took place in the early depositional stages of Unit 5, the suggested environment is quite a dynamic one, changing frequently between marsh and active streams. This environment presents a preferred setting for hominin activity; fresh water brought by the streams sustained a rich biotope where animals and plants could be obtained, both here and at the nearby marsh.

Together, the faunal remains from Evron Quarry (Tchernov et al., 1994) and the 'Evron Landfill locality, confirm the presence at the site of an impressive biogeographical mix comprising taxa originating from at least three different biogeographic provinces; Ethiopian (e.g., *E.* cf. *tabeti, Kolpochoerus,* and *Alcelaphus*), Oriental (e.g., *Elephas* sp. and *Stegodon* sp.) and Palaearctic (*Bos* sp. and Cervidae). As

https://doi.org/10.1017/qua.2018.107 Published online by Cambridge University Press

noted by Tchernov et al. (1994), it is unclear whether the African element in the Evron fauna represents a continuation of the early Pleistocene 'Ubeidiya dispersal event, or is a new post-'Ubeidiya occurrence. The presence of two grazers (an equid and a large bovid) as well as a cervid (browser) in the new finds suggests a mixed environment comprising open steppe as well as woodland. This supports the paleoecological reconstruction from the previous investigation at Evron Quarry (Tchernov et al., 1994) denoting a mosaic landscape of open, steppic country (*Gazella,* cf. *Alcelaphus*), woodlands (Cervidae, *Stegodon* sp., *Bos*. sp.), bare rocky slopes (cf. *Gerbillus* cf. *dayurus*), and water bodies (*Hippopotamus, Trionyx*) in close proximity to the site.

## CONCLUSIONS

A minimum age for the hominin activity in 'Evron Landfill was determined based on cosmogenic isotope burial age of the sediments overlaying the horizon from which archaeological finds originated, yielding an age of $0.66 \pm 0.11$ Ma. This result agrees with the paleomagnetic stratigraphy of the archaeological finds, which places it near the BM transition (ca. 0.77 Ma). A pedo-sedimentary study indicated that hominin activity primarily took place within a marsh environment, which was changing both spatially and temporally to an active stream, not far from the Mediterranean shore. Comparative analyses of the flint and faunal assemblages display similarities between the Landfill locality and the nearby Evron Quarry site, suggesting that this newly identified locality should be ascribed to the same cultural phase, i.e., the Early Acheulian.

## ACKNOWLEDGMENTS

The excavation at 'Evron Landfill was directed by Maayan Shemer (Field photography) and Omry Barzilai on behalf of the Israel Antiquity Authority (IAA; Permit A7414/2015), and was financed by Kibbutz 'Evron. Test trenches were conducted by Alla Yaroshevich. We thank Mrs. Argita Levanon and The National Laboratory for Digital Documentation of Archaeological Artifacts, for the digital documentation of selected flint artifacts found during the project; Mrs. Clara Amit for studio photographs of the finds and Mr. Mendel Kahn for map drafting and GPS documentation. The authors also would like to extend their gratitude to the IAA department of publications for permission granted to publish the assemblages collected during the excavation. In loving memory of Professor Avraham Ronen, an exceptional researcher and a dear colleague, excavator of Evron Quarry.

## SUPPLEMENTARY MATERIALS

To view supplementary material for this article, please visit https://doi.org/10.1017/qua.2018.107

## REFERENCES

Aguirre, E., Carbonell, E., 2001. Early human expansions into Eurasia: the Atapuerca evidence. *Quaternary International* 75, 11–18.

Argento, D.C., Reedy, R.C., Stone, J.O., 2013. Modeling the earth's cosmic radiation. *Nuclear Instruments and Methods in Physics Research Section B: Beam Interactions with Materials and Atoms* 294, 464–469.

Balco, G., Stone, J.O., Lifton, N.A., Dunai, T.J., 2008. A complete and easily accessible means of calculating surface exposure ages or erosion rates from $^{10}$Be and $^{26}$Al measurements. *Quaternary Geochronology* 3, 174–195.

Bar-Yosef, O., 1994. The Lower Paleolithic of the Near East. *Journal of World Prehistory* 8, 211–265.

Bar-Yosef, O., Belfer-Cohen, A., 2001. From Africa to Eurasia – early dispersals. *Quaternary International* 75, 19–28.

Bar-Yosef, O., Belfer-Cohen, A., 2013. Following Pleistocene road signs of human dispersals across Eurasia. *Quaternary International* 285, 30–43.

Bar-Yosef, O., Belmaker, M., 2011. Early and Middle Pleistocene faunal and hominins dispersals through Southwestern Asia. *Quaternary Science Reviews* 30, 1318–1337.

Bar-Yosef, O., Goren-Inbar, N., 1993. *The Lithic Assemblages of 'Ubeidiya: A Lower Palaeolithic Site in the Jordan Valley*. Institute of Archaeology, Hebrew University of Jerusalem, Jerusalem.

Barkai, R., Gopher, A., Lauritzen, S.E., Frumkin, A., 2003. Uranium series dates from Qesem Cave, Israel, and the end of the Lower Palaeolithic. *Nature* 423, 977–979.

Barzilai, O., Malinsky-Buller, A., Ackermann, O., 2006. Kefar Menachem West: a Lower Paleolithic site in the southern Shephela, Israel. *Journal of the Israel Prehistoric Society* 36, 7–38.

Bierman, P.R., Caffee, M., 2001. Slow rates of rock surface erosion and sediment production across the Namib Desert and escarpment, southern Africa. *American Journal of Science* 301, 326–358.

Buchbinder, B., 1975. Stratigraphic significance of the alga Amphiroa in Neogene-Quaternary bioclastic sediments. *Israel Journal of Earth-Sciences* 24, 44–48.

Chazan, M., 2013. Butchering with small tools: the implications of the Evron Quarry assemblage for the behavior of *Homo erectus*. *Antiquity* 87, 350–367.

Chmeleff, J., von Blanckenburg, F., Kossert, K., Jakob, D., 2010. Determination of the $^{10}$Be half-life by multicollector ICP-MS and liquid scintillation counting. *Nuclear Instruments and Methods in Physics Research Section B-Beam Interactions with Materials and Atoms* 268, 192–199.

Coltorti, M., Feraud, G., Marzoli, A., Peretto, C., Ton-That, T., Voinchet, P., Bahain, J.-J., Minelli, A., Hohenstein, U.T., 2005. New 40 Ar/39 Ar, stratigraphic and palaeoclimatic data on the Isernia la Pineta Lower Palaeolithic site, Molise, Italy. *Quaternary International* 131, 11–22.

Crouvi, O., Amit, R., Enzel, Y., Porat, N., Sandler, A., 2008. Sand dunes as a major proximal dust source for late Pleistocene loess in the Negev desert, Israel. *Quaternary Research* 70, 275–282.

Davis, M., Matmon, A., Rood, D.H., Avnaim-Katav, S., 2012. Constant cosmogenic nuclide concentrations in sand supplied from the Nile River over the past 2.5 my. *Geology* 40, 359–362.

Davis, S.J., 1980. Late Pleistocene and Holocene equid remains from Israel. *Zoological Journal of the Linnaean Society* 70, 289–312.

Debénath, A., Dibble, H.L., 1994. *Handbook of Paleolithic Typology: Lower and Middle Paleolithic of Europe, Vol. 1*. University of Pennsylvania, Museum of Archaeology, Philadelphia.

Eisenmann, V., 1986. Les Equidés d'Oubeidiyeh. In: Tchernov, E. and Guérin, C. (Eds.), *Les Mammifères du Pléistocène Inférieur de la Vallée du Jourdain à Oubeidiyeh.* Mémoires et Travaux du Centre de Recherche Français de Jérusalem, Vol. 5. Association Paléorient, Paris, pp. 191–212.

Eisenmann, V., 1992. Systematic and biostratigraphical interpretation of the equids from Qafzhe, Tabun, Shkul and Kebara (Acheulo-Yabrudian to Upper Paleolithic of Israel). *Archaeozoologica* 5, 43–62.

Eisenmann, V., 2012a. The Equids of Gesher Benot Ya'aqov, Israel (accessed August 2018). http://www.vera-eisenmann.com.

Eisenmann, V., 2012b. The Equids of Oumm Zinat, Israel (accessed August 2018). http://www.vera-eisenmann.com.

Eisenmann, V., Alberdi, M.T., De Giuli, C. Staesche, U., 1988. Studying fossil horses, volume I: methodology. In: Woodburne M.O., Sondaar, P.Y. (Eds.), *Collected Papers after the "New York International Hipparion Conference, 1981*." Brill, Leiden, pp. 1–71.

Garrod, D.A.E., 1956. 'Acheuleo-Jabrudian' et 'Pre-Aurignacian' de la grotte du Taboun (Mont Carmel): étude stratigraphique et chronologique. [In French.] *Quaternaria* 3, 39–59.

Garrod, D.A.E., 1970. Pre-Aurignacian and Amudian: a comparative study of the earliest blade industries of the Near East. In: Gripp, K., Schütrumpf, R., Schwabedissen, H. (Eds.), *Frühe Menschheit und Umwelt*. Böhlau Verlag, Köln, pp. 224–229.

Geraads, D., Tchernov, E., 1983. Femurs humains du Pleistocene Moyen de Gesher Benot Ya'aqov (Israel). [In French.] *L'Anthropologie* 87, 138–141.

Gilead, D., 1970. Handaxe industries in Israel and the Near East. *World Archaeology* 2, 1–11.

Gilead, D., Israel, M., 1975. An early Palaeolithic site at Kefar Menahem preliminary report. *Tel Aviv* 2, 1–12.

Gilead, D., Ronen, A., 1977. Acheulian industries from 'Evron on the western Galilee Coastal Plain. *Eretz-Israel* 13, 56–86.

Gopher, A., Ayalon, A., Bar-Matthews, M., Barkai, R., Frumkin, A., Karkanas, P., Shahack-Gross, R., 2010. The chronology of the late Lower Paleolithic in the Levant based on U–Th ages of speleothems from Qesem Cave, Israel. *Quaternary Geochronology* 5, 644–656.

Gopher, A., Barkai, R., Shimelmitz, R., Khalaily, M., Lemorini, C., Hershkovitz, I., Stiner, M., 2005. Qesem Cave: an Amudian site in central Israel. *Mitekufat Haeven: Journal of the Israel Prehistoric Society* 35, 69–92.

Goren-Inbar, N., Belitzky, S., Verosub, K., Werker, E., Kislev, M., Heimann, A., Carmi, I., Rosenfield, A., 1992. New discoveries at the Middle Pleistocene Acheulian site of Gesher Benot Ya'aqov, Israel. *Quaternary Research* 38, 117–128.

Goren-Inbar, N., Feibel, C.S., Verosub, K,L., Melamed, Y., Kislev, M.E., Tchernov, E., Saragusti, I., 2000. Pleistocene milestones on the out-of-Africa corridor at Gesher Benot Ya'aqov, Israel. *Science* 289, 944–974.

Goren-Inbar, N., Grosman, L., Sharon, G., 2011. The technology and significance of the Acheulian giant cores of Gesher Benot Ya'aqov, Israel. *Journal of Archaeological Science* 38, 1901–1917.

Goren-Inbar, N., Lister, A., Werker, E., Chech, M., 1994. A butchered elephant skull and associated artifacts from the Acheulian site of Gesher Benot Ya'aqov, Israel. *Paléorient* 20, 99–112.

Goren-Inbar, N., Speth, J.D., (Eds.), 2004. *Human Paleoecology in the Levantine Corridor*. Oxbow Books, Oxford.

Goring-Morris, A.N., Hovers, E., Belfer-Cohen, A., 2009. The dynamics of Pleistocene and Early Holocene settlement patterns and human adaptations in the Levant: an overview. In: Shea, J., Lieberman, D.E. (Eds.), *Transitions in Prehistory: Essays in Honor of Ofer Bar-Yosef*. Oxbow Book,s Oxford, pp. 185–252.

Granger, D.E., 2006. A review of burial dating methods using $^{26}$Al and $^{10}$Be. *Geological Society of America Special Paper* 415, 1.

Granger, D.E., Kirchner, J.W., Finkel, R.C., 1997. Quaternary downcutting rate of the New River, Virginia, measured from differential decay of cosmogenic 26Al and 10Be in cave-deposited alluvium. *Geology* 25, 107–110.

Granger, D., Muzikar, P., 2001. Dating sediment burial with in situ-produced cosmogenic nuclides: theory, techniques, and limitations. *Earth and Planetary Science Letters* 188, 269–281.

Guérin, C., Eisenmann, V., Faure, M., 1993. Les grands mammifères du gisement Pléistocène Moyen de Latamné (Valle de l'Oronte, Syrie). [In French.] In: Sanlaville, P., Bensacon, J., Copeland, L. and Muhesen, S. (Eds.), Le Paléolithic de la Valée Moyenne de l'Oronte (Syrie). British Archaeological Reports International Series, Vol. 587. Archaeopress, Oxford, pp. 169–178.

Gunz, P., Bookstein, F.L., Mitteroecker, P., Stadlmayr, A., Seidler, H., Webber, G.W., 2009. Early modern human diversity suggests subdivided population structure and a complex out-of-Africa scenario. *PNAS* 106, 6094–6098.

Gvirtzman, G., 1970. The Saqiye Group (Late Eocene to Early Pleistocene) in the Coastal Plain and the Hashefela regions. *Geological Survey of Israel Reports*, D/5/67.

Gvirtzman, G., Shachnai, E., Bakler, N., Ilani, S., 1984. Stratigraphy of the Kurkar Group (Quaternary) of the coastal plain of Israel. *Geological Survey of Israel Current Research*, 70–82.

Haas, G., 1970. *Metridiochoerus evronesis* N. Sp.: a new middle Pleistocene Phacochoerid from Israel. *Israel Journal of Zoology* 19, 179–181.

Herzlinger, G., Wynn, T., Goren-Inbar, N., 2017. Expert cognition in the production sequence of Acheulian cleavers at Gesher Benot Ya'aqov, Israel: a lithic and cognitive analysis. *PLoS ONE* 12, e0188337. http://dx.doi.org/10.1371/journal.pone.0188337

Hidy, A.J., Gosse, J.C., Blum, M.D., Gibling, M.R., 2014. Glacial–interglacial variation in denudation rates from interior Texas, USA, established with cosmogenic nuclides. *Earth and Planetary Science Letters* 390, 209–221.

Hooijer, D.A., 1959. Fossil mammals from Jisr Banat Yaqub, south of Lake Hule, Israel. *Bulletin of the Research Council of Israel* G8, 177–179.

Horwitz, L.K., Chazan, M., 2007. Holon in the context of the Levantine Lower Paleolithic. In: Chazan, M., Horwitz, L.K. (Eds.), *The Lower Paleolithic Site of Holon, Israel*. American School of Prehistoric Research Bulletin 50, Peabody Museum of Archaeology and Ethnology. Harvard University Press, Cambridge, pp. 181–191.

Horwitz, L.K., Monchot, H., 2007. *Sus, Hippopotamus, Bos*, and *Gazella*. In: Chazan, M., Horwitz, L.K., (Eds.), *The Lower Paleolithic Site of Holon, Israel*. American School of Prehistoric Research Bulletin 50, Peabody Museum of Archaeology and Ethnology. Harvard University Press, Cambridge, pp. 91–109.

Horwitz, L.K., Tchernov, E., 1989. The Late Acheulian fauna from Oumm Zinat. *Journal of the Israel Prehistoric Society* 22, 7–14.

Issar, A., Kafri, U., 1969. The discovery of Pleistocene mammalian fauna and artifacts at Evron, western Galilee, Israel. *Journal of Earth Sciences* 18, 147.

Jelinek, A.J., 1990. The Amudian in the context of the Mugharan tradition at the Tabun cave (Mt. Carmel), Israel. In: Mellars, P. (Ed.), *The Emergence of Modern Humans*. Edinburgh University Press, Edinburgh, pp. 81–90.

Kafri, U., Ecker, A. 1964. Neogene and Quaternary subsurface geology and Hydrogeology of the Zevulun Plain. *Geological Survey of Israel Bulletin* 37, 13 pp.

Kohl, C., Nishiizumi, K., 1992. Chemical isolation of quartz for measurement of in-situ-produced cosmogenic nuclides. *Geochimica et Cosmochimica Acta* 56, 3583–3587.

Korschinek, G., Bergmaier, A., Faestermann, T., Gerstmann, U., Knie, K., Rugel, G., Wallner, A., Dillmann, I., Dollinger, G., Von Gostomski, C.L., 2010. A new value for the half-life of $^{10}$Be by Heavy-Ion Elastic Recoil Detection and liquid scintillation counting. *Nuclear Instruments and Methods in Physics Research Section B: Beam Interactions with Materials and Atoms* 268, 187–191.

Lifton, N., Sato, T., Dunai, T.J., 2014. Scaling *in situ* cosmogenic nuclide production rates using analytical approximations to atmospheric cosmic-ray fluxes. *Earth and Planetary Science Letters* 386, 149–160.

Lister, A.M., Dirks, W., Assaf, A., Chazan, M., Goldberg, P., Applbaum, J., Greenbaum, N., Horwitz, L.K., 2013. New fossil remains of *Elephas* from the southern Levant, and the evolutionary history of the Asian elephant. *Palaeogeography, Palaeoclimatology, Palaeoecology* 386, 119–130.

Malinsky-Buller, A., Hovers, E., Marder, O., 2011. Making time: 'living floors','palimpsests' and site formation processes–A perspective from the open-air Lower Paleolithic site of Revadim Quarry, Israel. *Journal of Anthropological Archaeology* 30, 89–101.

Malinsky-Buller, A., Barzilai, O., Ayalon, A., Bar-Matthews, M., Birkenfeld, M., Porat, N., Ron, H., Ackermann, O., 2016. The age of the Lower Paleolithic site of Kefar Menachem West, Israel—another facet of Acheulian variability. *Journal of Archaeological Science: Reports* 10, 350–362.

Marder, O., Malinsky-Buller, A., Shahack-Gross, R., Ackermann, O., Ayalon, A., Bar-Matthews, M., Goldsmith, Y., Inbar, M., Rabinovich, R., Hovers, E., 2011. Archaeological horizons and fluvial processes at the Lower Paleolithic open-air site of Ravadim (Israel). *Journal of Human Evolution* 60, 508–522.

Martínez-Navarro, B., Belmaker, M., Bar-Yosef, O., 2009. The large carnivores from 'Ubeidiya (early Pleistocene, Israel): biochronological and biogeographical implications. *Journal of Human Evolution* 56, 514–524.

Martínez-Navarro, B., Belmaker, M., Bar-Yosef, O., 2012. The Bovid assemblage (Bovidae, Mammalia) from the early Pleistocene site of 'Ubeidiya, Israel: biochronological and paleoecological implications for the fossil and lithic bearing strata. *Quaternary International* 267, 78–97.

Martínez-Navarro, B., Rabinovich, R., 2011. The fossil Bovidae (Artiodactyla, Mammalia) from Gesher Benot Ya'aqov, Israel: out of Africa during the early-middle Pleistocene transition. *Journal of Human Evolution* 60, 375–386.

Matmon, A., Fink, D., Davis, M., Niedermann, S., Rood, D., Frumkin, A., 2014. Unraveling rift margin evolution and escarpment development ages along the Dead Sea fault using cosmogenic burial ages. *Quaternary Research* 82, 281–295.

Mishra, S., Venkatesan, T.R., Rajaguru, S.N., Somayajulu, B.L.K., 1995. Earliest Acheulian industry from peninsular India. *Current Anthropology* 36, 847–851.

Neuville, R., 1951. *Le Paléolithique et le Mésolithique du désert de Judée*. Archives de l'Institut de paléontologie humain 24. Masson, Paris.

Nishiizumi, K., 2004. Preparation of $^{26}$Al AMS standards. *Nuclear Instruments and Methods in Physics Research Section B: Beam Interactions with Materials and Atoms* 223, 388–392.

Nishiizumi, K., Imamura, M., Caffee, M.W., Southon, J.R., Finkel, R.C., McAninch, J., 2007. Absolute calibration of $^{10}$Be AMS standards. *Nuclear Instruments and Methods in Physics Research Section B: Beam Interactions with Materials and Atoms* 258, 403–413.

Norton, C.J., Bae, K., Harris, J.W., Lee, H., 2006. Middle Pleistocene handaxes from the Korean peninsula. *Journal of Human Evolution* 51, 527–536.

Porat, N., Chazan, M., Schwarcz, H., Horwitz, L.K., 2002. Timing of the Lower to Middle Paleolithic boundary: New dates from the Levant. *Journal of Human Evolution* 43, 107–122.

Porat, N., Ronen, A., 2002. Luminescence and ESR age determinations of the Lower Paleolithic site Evron Quarry, Israel. *Advances in ESR Applications* 18,123–130.

Porat, N., Zhou, L.P., Chazan, M., Noy, T., Horwitz, L.K., 1999. Dating the Lower Paleolithic open-air site of Holon, Israel by luminescence and ESR techniques. *Quaternary Research* 51, 328–341.

Prausnitz, M.W., 1969. The sequence of Early to Middle Paleolithic flint industries along the Galilean littoral. *Israel Exploration Journal* 19, 129–136.

Rabinovich, R., Ackermann, O., Aladjem, E., Barkai, R., Biton, R., Milevski, I., Solodenko, N., Marder, O., 2012. Elephants at the Middle Pleistocene Acheulian open-air site of Revadim Quarry, Israel. *Quaternary International* 276–277, 183–197.

Rabinovich, R., Gaudzinski-Windheuser, S., Kindler, L., Goren-Inbar, N., 2011. The Acheulian Site of Gesher Benot Ya'aqov Volume III: Mammalian Taphonomy. The Assemblages of Layers V-5 and V-6. Springer, Dordrecht.

Rech, J.A., Quintero, L.A., Wilke, P.J., Winer, E.R., 2007. The lower paleolithic landscape of 'Ayoun Qedim, al-Jafr Basin, Jordan. *Geoarchaeology: An International Journal* 22, 261–275.

Reiss, Z., Issar, A., 1961. Subsurface Quaternary correlations in the Tel Aviv region. *Geological Survey of Israel Bulletin* 32, 10–26.

Reynaud-Savioz, N., 2011. The faunal remains from Nadaouiyeh Aïn Askar (Syria). Preliminary indications of animal acquisition in an Acheulean site. In: le Tensorer, J.-M., Jagher, R., Otte, M. (Eds.), *The Lower and Middle Palaleolithic in the Middle East and Neighbouring Regions*. Etudes et Recherches archéologiques de l Université de Liége 126. Université de Liége, Liège, pp. 225–233.

Rink, W.J., Schwarcz, H.P., 2005. ESR and Uranium series dating of teeth from the Lower Paleolithic site of Gesher Benot Ya'aqov, Israel: Confirmation of paleomagnetic age indications. *Geoarchaeology* 20, 57–66.

Rollefson, G.O., Quintero, L.A., Wilke, P.J., 2006. Late Acheulian variability in the southern Levant: a contrast of the western and eastern margins of the Levantine Corridor. *Near Eastern Archaeology* 69, 61.

Rollefson, G., Schnurrenberger, D., Quintero, L., Watson, R.P., Low, R., 1997. Ain Soda and 'Ayn Qasiya: new late Pleistocene and early Holocene sites in the Azraq Shishan area, eastern Jordan. In: Gebel, H.G., Kafafi, Z., Rollefson, G.O., (Eds.), *The*

https://doi.org/10.1017/qua.2018.107 Published online by Cambridge University Press

*Prehistory of Jordan, Vol. II: Perspectives from 1997*. Ex Oriente, Berlin, pp. 45–58.

Ron, H., Porat, N., Ronen, A., Tchernov, E., Horwitz, L.K., 2003. Magnetostratigraphy of the Evron Member-implications for the age of the Middle Acheulian site of Evron Quarry. *Journal of Human Evolution* 44, 633–639.

Ronen, A., 1979. Paleolithic industries in Israel. In: Horowitz, A. (Ed.), *The Quaternary of Israel*. Academic Press, New York, pp. 296–307.

Ronen, A., 1991. The Lower Palaeolithic site Evron-Quarry in western Galilee, Israel. *Sonderveröffentlichungen Geologisches Institut der Universität zu Köln* 82, 187–212.

Ronen, A., 1993. 'Evron-the prehistoric sites. In: Stern, E., Lewinson-Gilboa, A., Aviram, J. (Eds.), *The New Encyclopedia of Archaeological Excavations in the Holy Land.* Vol. 3. The Israel Exploration Society and Carta, Jerusalem, pp. 430–431.

Ronen, A., Amiel, A., 1974. The Evron Quarry: a contribution to the Quaternary stratigraphy of the coastal plain of Israel. *Paléorient* 2, 167–173.

Ronen, A., Prausnitz, M., 1979. Excavations at a Paleolithic hunters'-site in the Evron quarry. [In Hebrew.] *Qadmoniot* 2/3, 51–53.

Ronen, A., Winter, Y., 1997. Eyal 23: a Lower Palaeolithic site in the eastern Sharon, Israel. *Quartär* 47, 177–188.

Sanlaville, P., Bensacon, J., Copeland, L. and Muhesen, S. (Eds.), 1993. Le Paléolithic de la Valée Moyenne de l'Oronte (Syrie). *BAR International Series*, Vol. 587. Oxford: Archaeopress.

Saragusti, I., Goren-Inbar, N., 2001. The biface assemblage from Gesher Benot Ya'akov, Israel: illuminating patterns in "out of Africa" dispersal. *Quaternary International* 75, 85–89.

Sharon, G., 2007. *Acheulian Large Flake Industries: Technology, Chronology, and Significance*. Archaeopress, Oxford.

Sharon, G., 2014. The early prehistory of Western and Central Asia. In: Renfrew C., Bahn, P., (Eds.), *The Cambridge World Prehistory*. Cambridge University Press, Cambridge, pp. 1357–1378.

Shea, J.J., 1999. Artifact abrasion, fluvial processes, and "living floors" from the Early Paleolithic site of'Ubeidiya (Jordan Valley, Israel). *Geoarchaeology* 14, 191–207.

Shemer, M., Barzilai, O., 2017. 'Evron (East). Hadashot Arkheologiyot, excavations and surveys in Israel 129 (accessed August 24, 2017). http://www.hadashot-esi.org.il/report_detail.aspx?id=25165& mag_id=125

Singer, B.S., 2014. A Quaternary geomagnetic instability time scale. *Quaternary Geochronology* 21, 29–52.

Sivan, D., 1995. *Paleogeography of the Galilee Coastal Plain during the Quaternary*. Unpublished PhD Thesis, The Hebrew University, Jerusalem (in Hebrew, English abstract).

Sivan, D., 1996. Paleogeography of the Galilee coastal plain during the Quaternary. Geological Survey of Israel Reports GSI/18/96 (in Hebrew).

Sivan, D., Gvirtzman, G., Sass, E., 1999. Quaternary stratigraphy and paleogeography of the Galilee coastal plain, Israel. *Quaternary Research* 51, 280–294.

Sivan, D., Wdowinski, S., Lambeck, K., Galili, E., Raban, A., 2001. Holocene sea-level changes along the Mediterranean coast of Israel, based on archaeological observations and numerical model. *Palaeogeography, Palaeoclimatology, Palaeoecology* 167, 101–117.

Slott-Moller, R., 1990. La faune. In: Jaubert, J., Lorblanchet, M. (Eds.), *Les Chasseurs d'Aurochs de la Borde. Un site du Paléolithique moyen (Livernon, Lot)*. Documents d'Archéologie Française vol. 27. Editions de la Maison des Sciences de l'Homme, Paris. pp. 33–68.

Soil Survey Staff, 1999. *Soil Taxonomy: A Basic System of Soil Classification for Making and Interpreting Soil Surveys*. United States Government Printing Office, Washington, DC.

Stekelis, M., 1950. 'Evron. [In Hebrew.] *Bulletin of the Department of Antiquities of the State of Israel* 2, 29–30.

Stekelis, M., Gilead, D., 1966. Maayan Baruch, a Lower Palaeolithic Site in Upper Galilee. *Mitekufat Haeven* 8, 1–23.

Stiner, M.C., Barkai, R., Gopher, A., 2009. Cooperative hunting and meat sharing 400–200 kya at Qesem Cave, Israel. *Proceedings of the National Academy of Sciences of the United States of America* 106, 13207–13212.

Stone, J.O., 2000. Air pressure and cosmogenic isotope production. *Journal of Geophysical Research* 105, 23753–23759.

Tauxe, L., Shaar, R., Jonestrask, L., Swanson-Hysell, N.L., Minnett, R., Koppers, A.A.P., Constable, C.G, Jarboe, N., Gaastra, K., Fairchild, L., 2016. PmagPy: software package for paleomagnetic data analysis and a bridge to the Magnetics Information Consortium (MagIC) Database. *Geochemistry, Geophysics, Geosystems* 17, 2450–2463.

Tchernov, E., 1987. The age of the Ubeidiya Formation, an early Pleistocene hominid site in the Jordan valley, Israel. *Israel Journal of Earth Sciences* 36, 3–30.

Tchernov, E., 1992. Biochronology, paleoecology, and dispersal events of hominids in the southern Levant. In: Akazawa, T., Aoki, K., Kimura, T. (Eds.), *The Evolution and Dispersal of Modern Humans in Asia*. Hokusen-sha, Tokyo, pp. 149–188.

Tchernov, E., Horwitz, L.K., Ronen, A., Lister, A., 1994. The faunal remains from Evron Quarry in relation to other Lower Paleolithic hominid sites in the southern Levant. *Quaternary Research* 42, 328–339.

Templeton, A., 2002. Out of Africa again and again. *Nature* 416, 45–51.

Valladas, H., Mercier, N., Hershkovitz, I., Zaidner, Y., Tsatskin, A., Yeshurun, R., Vialettes, L., Joron, J.-L., Reyss, J.-L., Weinstein-Evron, M., 2013. Dating the Lower to Middle Paleolithic transition in the Levant: a view from Misliya Cave, Mount Carmel, Israel. *Journal of Human Evolution* 65, 585–593.

Weinstein-Evron, M., Bar-Oz, G., Zaidner, Y., Tsatskin, A., Druck, D., Porat, N., Hershkovitz, I., 2003. Introducing Misliya cave, Mount Carmel, Israel: a new continuous Lower/Middle Paleolithic sequence in the Levant. *Eurasian Prehistory* 1, 31–55.

Weinstein-Evron, M., Tsatskin, A., Porat, N., Kronfeld, J., 1999. A 230Th/234U date for the Acheulo-Yabrudian layer in the Jamal Cave, Mount Carmel, Israel. *South African Journal of Sciences* 95, 186–188.

Yeshurun, R., Zaidner, Y., Eisenmann, V., Martínez-Navarro, B., Bar-Oz, G., 2011. Lower Paleolithic hominin ecology at the fringe of the desert: faunal remains from Bizat Ruhama and Nahal Hesi, Northern Negev, Israel. *Journal of Human Evolution* 60, 492–507.

Yisraeli, T., 1967. A Lower Palaeolithic site at Holon: preliminary report. *Israel Exploration Journal* 17, 144–152.

Zaidner, Y., 2014. *Lithic production strategies at the early Pleistocene site of Bizat Ruhama, Israel*. Archaeopress, CITY.

Zaidner, Y., Porat, N., Zilberman, E., Herzlinger, G., Almogi-Labin, A., Roskin, J., 2018. Geo-chronological context of the open-air Acheulian site at Nahal Hesi, northwestern Negev, Israel. *Quaternary International* 464, 18–31.

https://doi.org/10.1017/qua.2018.107 Published online by Cambridge University Press

Zaidner, Y., Ronen, A., Burdukiewicz, J.M., 2003. L'industrie microlithique du Paléolithique inférieur de Bizat Ruhama, Israël. *L'Anthropologie* 107, 203–222.

Zijderveld, J.D.A., 1967. A.C. demagnetization of rocks: analysis of results, In: D.W. Collinson, K M. Creer and S.K. Runcorn (Eds.), *Methods in Palaeomagnetism*. Elsevier, Amsterdam and New York, pp. 254–286.

Zilberman, E., 1991. Landscape evolution in the central, northern and northwestern Negev during the Neogene and the Quaternary. *Geolgical Survey of Israel Reports* GSI/45/90.

https://doi.org/10.1017/qua.2018.107 Published online by Cambridge University Press